DRA

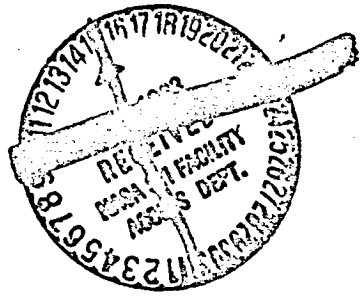

FINAL REPORT

for

GRANT NAG 5-106

from the

NATIONAL AERONAUTICS AND SPACE ADMINISTRATION

For the period 9/15/80 to 5/15/83

PARAMETERIZATION OF CLOUD EFFECTS ON THE ABSORPTION OF SOLAR RADIATION

ROGER DAVIES, Principal Investigator

Department of Geosciences
Purdue University
West Lafayette, Indiana 47907

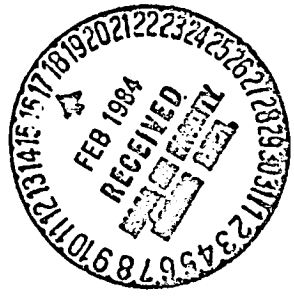

(NASA-CR-175154) PARAMETERIZATION OF CLOUD EFFECTS ON THE ABSORPTION OF SOLAR RADIATION Final Report, 15 Sep. 1980 - 15 May 1983 (Purdue Univ.) 99 p HC A05/MF A01 CSCL 04B

N84-16712

G3/47 Unclas 10153

#

N84-16712

INTRODUCTION

As we attempt to better understand the causal mechanisms of climate and climate change through the development of comprehensive general circulation models, greater demands are placed on our representation of the relevant physical processes. Unlike short term prediction models, where the accumulation of biases in slowly acting forces may be of little practical consequence, climate models require a careful accounting of all terms that affect the energy budget of a region. Foremost amongst these, and the source of the energy that drives the subsequent atmospheric motion, is the term related to the absorption of solar radiation.

This final report describes the results of research on the absorption of solar radiation, carried out under grant NAG 5-106 from the National Aeronautics and Space Administration, which provided support of approximately $78,679 over a period of two and a half years. A number of connected studies were performed, including the development of a new parameterization scheme for the absorption of solar radiation, experiments with a comprehensive general circulation model, and development of a new theoretical model of the absorption of solar radiation in clouds. The report is consequently divided into three parts.

Part one is an abstract of NASA TECHNICAL MEMORANDUM 83961 ("Documentation of the solar radiation parameterization in the GLAS climate model". R. Davies, 1982, 57pp.), which describes the early phase of this research on the development, testing and implementation of a new radiation parameterization for the NASA Goddard Space Flight Center's climate model.

Part two is a summary of interactive and off-line experiments with the climate model to determine the limitations of the present parameterization scheme, culminating in suggestions for future improvements.

Part three lays the theoretical groundwork for one of the suggested improvements, namely the parameterization of cloud absorption in terms of solar zenith angle, column water vapor above the cloud top, and cloud liquid water content. This part describes research which led to a Master of Science degree for Mr. Kyung-Eak Kim, under the supervision of the Principal Investigator, and forms the bulk of the report.

PART I

Abstracted from NASA TECHNICAL MEMORANDUM 83961, entitled:

DOCUMENTATION OF THE SOLAR RADIATION PARAMETERIZATION IN THE GLAS CLIMATE MODEL,

by R. Davies, June, 1982.

This document describes the parameterization of solar radiation in the GLAS GCM. The parameterization is a revision of the Lacis-Hansen parameterization; it explicitly considers the directional nature of the direct solar beam in treating radiative transfer within clouds, and in treating the effect of surface reflection. This is accomplished using delta-Eddington and delta-two stream models for the radiative transfer within isolated atmospheric layers, and by coupling the individual layers together by efficiently repeated applications of the interaction principle.

Off-line comparisons with the previous non-directional, or diffuse, model yield significant differences in the planetary albedo and in the amounts of absorbed solar radiation. These differences show a systematic dependence on latitude and season.

PART II

PRESENT PARAMETERIZATION OF SOLAR RADIATION IN THE GODDARD CLIMATE MODEL

An enhancement to the solar radiation parameterization in the Goddard climate model, together with comparative results from the earlier version developed by Lacis and Hansen (1974), was described in detail by Davies (1982). Briefly, this enhancement provides a physically more realistic treatment of radiative transfer within clouds and at the earth's surface, as verified by comparison with more comprehensive models, specifically taking into account dependence on the directionality of the direct solar beam. This dependence produced differences in the absorption of solar radiation which varied more or less systematically from equator to pole, perturbed by cloud variability.

Since then, fully interactive comparisons have been made using the complete global climate model, yielding differences which are generally consistent with the off-line results. Their significance, however, is harder to interpret due to the presently fixed sea surface temperatures and unspecified model noise of the fully interactive model. Fig. 1, for example, shows differences in the monthly mean ground temperatures using the two parameterization schemes, showing that the climate model did appear to respond to the change in the parameterization.

An important consideration in parameterizing solar radiation is the question of the required accuracy of the parameterization scheme. While this question has yet to be seriously answered, the required accuracy presumably depends on the time scale of the application and on the type of error, random errors being more tolerable than those which show

persistent latitudinal or vertical biases. To obtain a nominal figure for the required accuracy of the solar parameterization scheme in the Goddard climate model, the atmospheric solar absorption was systematically perturbed during an interactive model run, and the effect on mean monthly atmospheric temperatures was analyzed. It was found that a change in the mean monthly, globally averaged, atmospheric temperature of 0.5K was produced by a systematic perturbation of ~ 7 Wm^{-2} in absorbed solar radiation. This amount was then taken as a nominal goal for the required accuracy of the parameterization scheme.

The next consideration was whether or not the radiation parameterization attains the above goal, and a number of off-line experiments were performed to this end. For clear sky cases, there was no evidence of systematic errors exceeding a few watts per square meter, the uncertainty in the absorbed radiation being mainly due to the uncertainty in the input variables of surface albedo, water vapor and ozone. Potentially large systematic errors appear to exist for cloudy regions, however, as illustrated in Fig. 2. This figure shows the differences in monthly mean absorbed solar energy obtained in an off-line experiment in which the treatment of cloud optical thickness was changed.

Instead of using a continuous cloud cover with constant optical thickness across the whole area of each cloud grid element, the experimental treatment assumed a cloud fraction of 0.45 whenever the climate model generated convective cloud for the grid element. The optical thickness of the cloudy fraction of each relevant level was then increased to give the same area-averaged optical thickness as before. Since area-averaged transmission, in particular, depends on optical thickness in a highly non-linear manner, and this dependence is also sensitive to solar zenith angle, the differences obtained are

not surprising and serve to illustrate the potential errors in the present scheme. The sensitivity to fractional cloud effects is particularly evident in the tropics and subtropics due to the frequency of convective clouds and small solar zenith angles at these latitudes. The typical discrepancy in the total solar absorption for these latitudes is ~ 35 Wm^{-2}, which is approximately a 10% effect and well above the nominal threshold of ~ 7 Wm^{-2}.

In terms of the evolution of the present parameterization, the next step should be a study of this fractional cloud effect in more detail with a view to reducing the latitudinal biases in absorbed solar radiation. Since a formal solution to the broken cloud problem, involving distributions of cloud sizes, shapes, liquid water contents, etc. is beyond the scope of the climate model, as presently planned, the new parameterization should be limited to functional dependences on cloud fraction, cloud temperature and solar zenith angle. These parameterizations could be obtained in part through the analysis of more rigorous cloud modeling as described in Part III.

For example, Fig. 3 shows preliminary results for the total absorption of solar radiation by a 1 km thick cloud as a function of cloud top height, assuming the droplet size-distribution remains constant. The cloud is embedded in a tropical maritime atmosphere with overhead sun. The total cloud absorption rises uniformly with increasing cloud altitude as the column water vapor above the cloud decreases and absorbs less of the solar infrared. Most of the cloud absorption is due to liquid water and not the water vapor within the cloud. In fact the cloud water vapor only contributes 10-20% of the total cloud absorption, and remains relatively constant with cloud top altitude. This is because the effect of increased solar infrared at higher altitudes is offset by less water

vapor within the cloud due to colder cloud temperatures.

These results indicate that the present parameterization of the transfer of solar infrared radiation in clouds should be substantially revised on physical grounds to reflect the dominant role of cloud droplets on absorption. Despite the extensive computational effort required for their production, the results obtained do not show any especially complex dependence on cloud height, temperature and solar zenith angle. It should therefore be possible to parameterize them in a straightforward manner.

References

1. Davies, R., 1982: Documentation of the solar radiation parameterization in the GLAS climate model. *NASA TECH. MEM.* 83961. 57pp.

2. Lacis, A.A., and J.E. Hansen, 1974: A parameterization for the absorption of solar radiation in the earth's atmosphere. *J. Atmos. Sci.*, 118-133.

Figure Captions

Fig. 1. Differences (revised minus original) in ground temperature from two interactive runs of the Goddard general circulation climate model, using, respectively, the revised and original solar radiation parameterizations. July averages.

Fig. 2. Differences (experimental treatment of cloud fraction minus standard treatment) in zonally averaged system absorption of solar radiation. The standard treatment assumes 100% cloud cover when cloud is present. The experimental treatment assumes 45% cloud cover with greater optical thickness, if convective cloud is present in the grid element. Single time step in mid-April.

Fig. 3. Results from a comprehensive radiative transfer model for absorbed solar radiation as a function of cloud top altitude for constant cloud thickness of 1 km. Moist tropical atmosphere with overhead sun.

(a) Absorption by water vapor within cloud.

(b) Absorption by cloud droplets.

(c) Total cloud absorption.

(d) Absorption by water vapor above cloud.

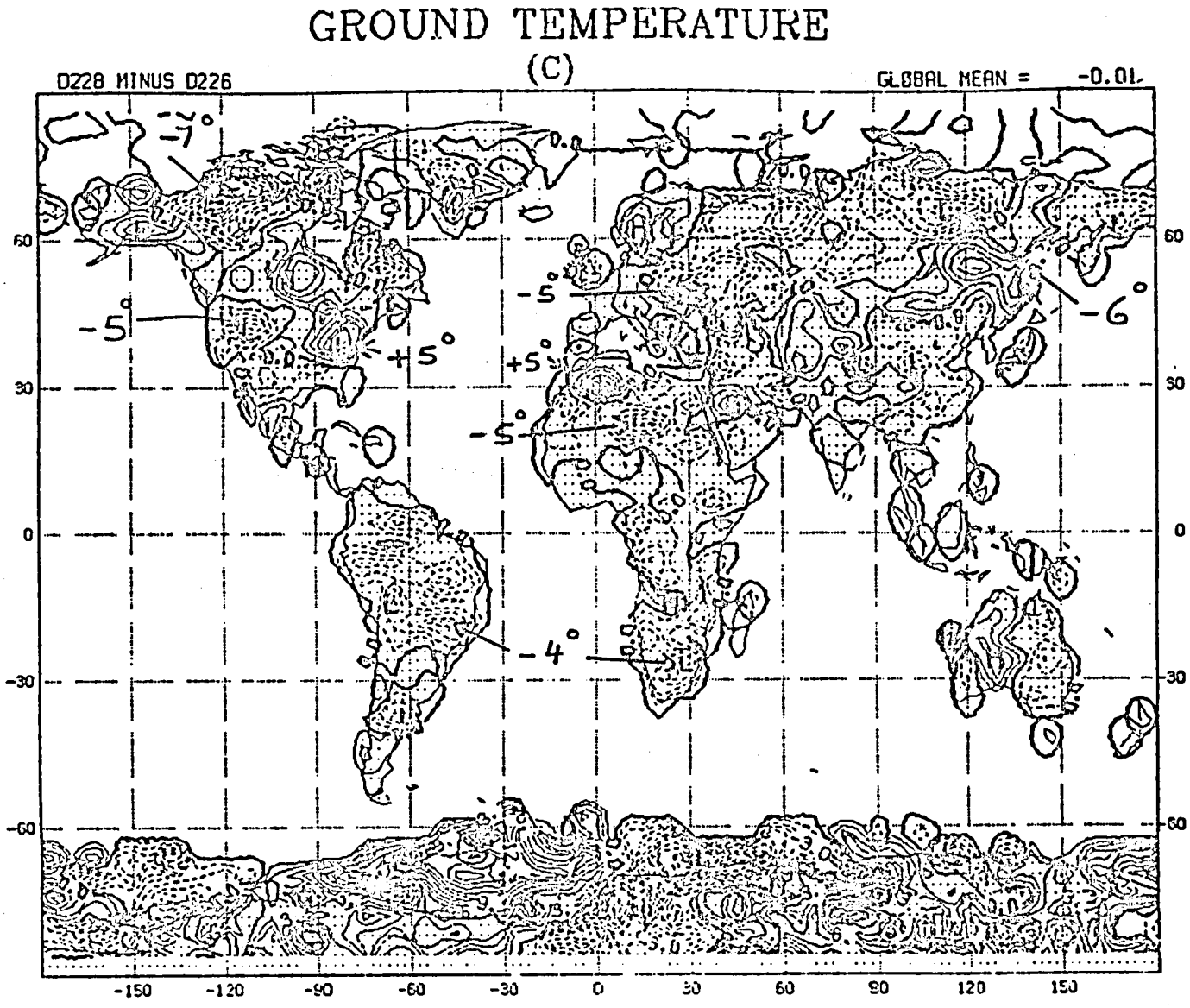

Figure 1

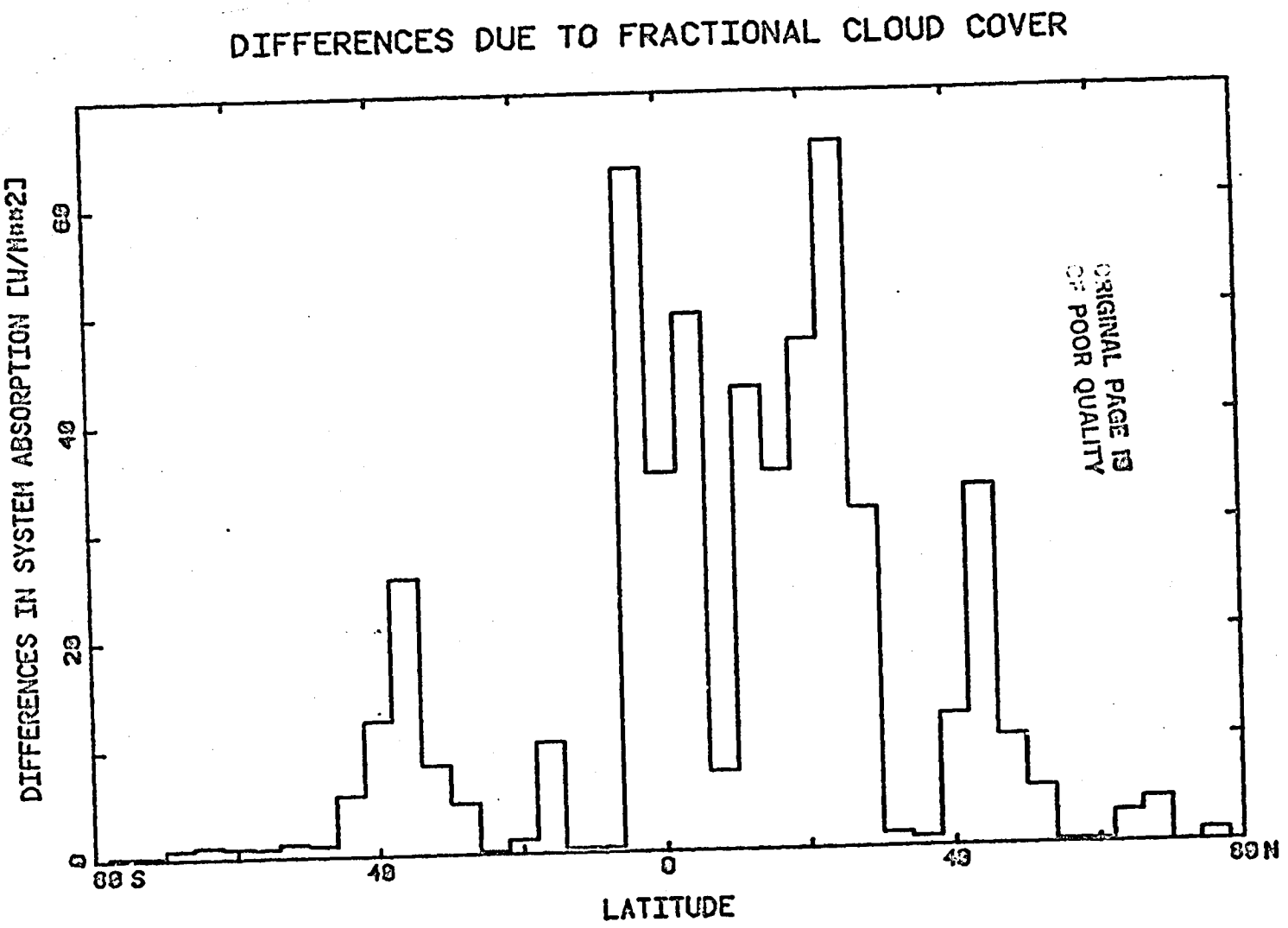
DIFFERENCES DUE TO FRACTIONAL CLOUD COVER
DIFFERENCES IN SYSTEM ABSORPTION [W/M**2]
0
20
40
60
80 S
40
0
40
80 N
LATITUDE
ORIGINAL PAGE IS
OF POOR QUALITY

Figure 2

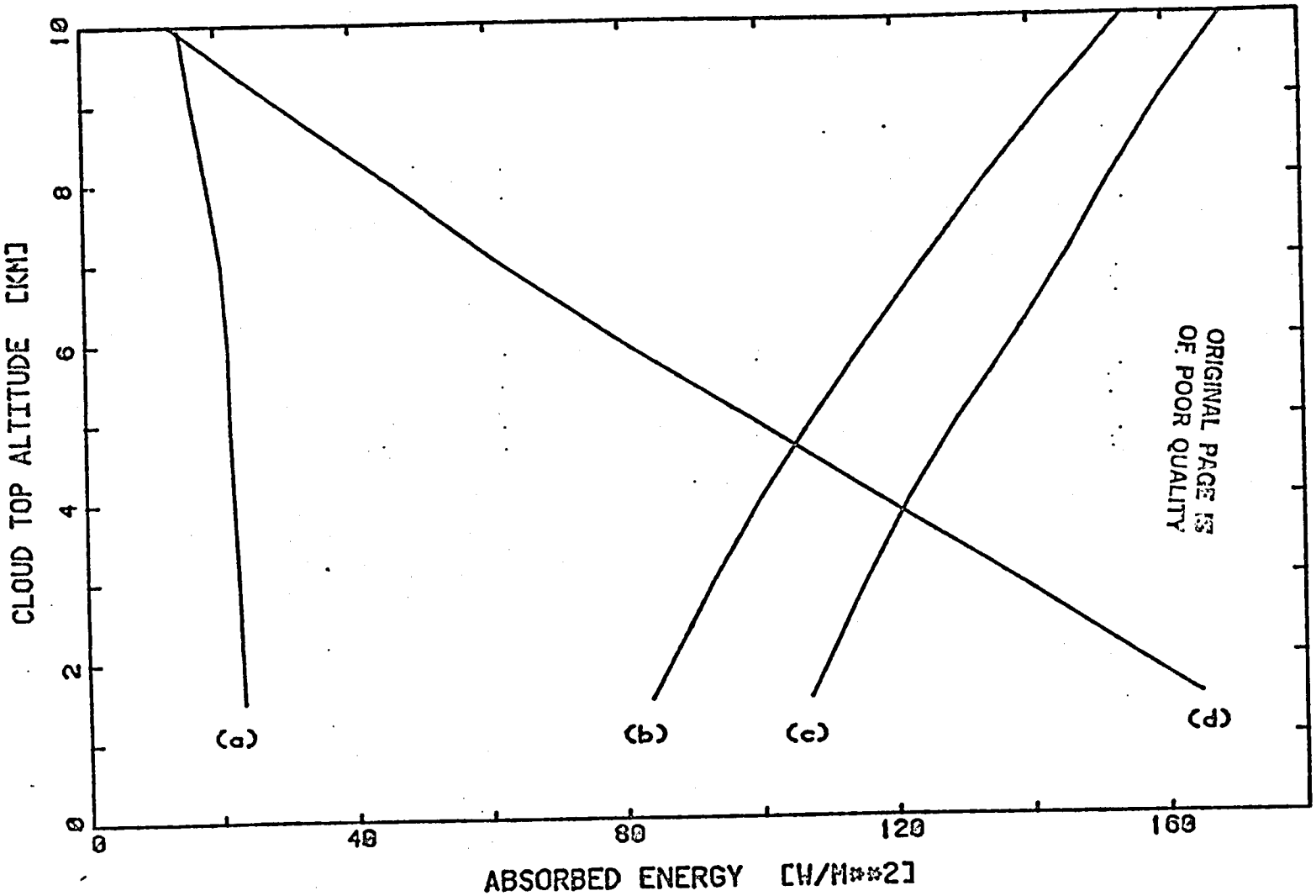
CLOUD TOP ALTITUDE [KM]
0
2
4
6
8
10
0
40
80
120
160
ABSORBED ENERGY [W/M**2]
(a)
(b)
(c)
(d)
ORIGINAL PAGE IS
OF POOR QUALITY

Figure 3

PART III

SPECTRAL ABSORPTION OF SOLAR RADIATION IN HOMOGENEOUS CLOUDS

A Thesis

Submitted to the Faculty

of

Purdue University

by

Kyung-Eak Kim

In Partial Fulfillment of the

Requirement for the Degree

of

Master of Science

August 1983

ACKNOWLEDGEMENTS

I would like to express sincere gratitude and appreciation to my major professor, Dr. Roger Davies, for his guidance and financial support through this work. His many helpful comments and suggestions greatly aided my research efforts and enabled me to conduct thorough investigations.

I am grateful to my committee including Dr. Phillip J. Smith and Dr. Dayton G. Vincent for their helpful suggestions of this manuscript. Also, my special thanks are extended to Dr. William L. Ridgway for making available pathlength distribution data obtained by Monte Carlo simulation, and useful plotting routines. His many helpful comments and suggestions greatly improved my understanding in the problem of this thesis.

The author wishes to express his appreciation to Dr. W. Wiscombe for a copy of his computer program for the calculation of Mie optical parameters.

I would like to express my thanks to my friend, Dr. Chang-eob Baag for his continuous encouragement and help since I came to America in August 1980.

I appreciate deeply my parents and wife's parents for their many sacrifices endured to allow me to finish this work.

Finally, the author wishes to express his sincere gratitude to his wife, Gil-Ryang Byun for her enccuragement and help during the course of this study.

This research was partially supported by the National Aeronautics and Space Administration under grant NAG 5-106.

TABLE OF CONTENTS

Page

LIST OF TABLES

LIST OF FIGURES

Figure Page

ABSTRACT

Kim, Kyung-Eak. M.S., Purdue University, August 1983. Spectral Absorption of Solar Radiation in Homogeneous Clouds. Major Professor: Dr. Roger Davies.

In order to better estimate total cloud absorption, spectral cloud absorption and the relative role of liquid water and water vapor, a theoretical model of a plane-parallel homogeneous cloud has been developed. This model uses a photon pathlength distribution to include the effects of multiple scattering. The water vapor transmission function is obtained from LOWTRAN 5.

The results indicate that 1 km thick clouds absorb about 8 to 12 % of solar radiation incident on the cloud top, and cloud absorption is highly dependent upon the wavenumber. Cloud absorption between 1500 cm^{-1} and 7500 cm^{-1} is primarily due to liquid water while cloud absorption between 11500 cm^{-1} and 15000 cm^{-1} is due to water vapor absorption. Over the spectral range 7500 cm^{-1} to 11500 cm^{-1}, both liquid water and water vapor are responsible for cloud absorption. In terms of relative absorption, liquid water contributes about 77 to 91 % of total cloud absorption, depending on cloud type, cloud top altitude, solar zenith angle, and atmospheric

model, while cloud water vapor contributes the remaining 9 to 23 %.

As cloud top altitude increases, the amount of energy absorbed by cloud and liquid water increases significantly while the amount of energy absorbed by water vapor is nearly constant. The absorption by atmospheric water vapor above the cloud strongly affects the amount of energy absorbed by the cloud, and should not be neglected in the calculation of cloud absorption. The fractional absorption by a cloud does not show significant differences for different seasonal and zonal atmospheric models.

The application of the model results suggest that the global average of cloud absorption is about 8 to 9 % of the incident solar radiation on the cloud top, based on the global estimation of liquid water content and cloud thickness. The global mean fractional cloud absorption is about 7 % of the global average of solar irradiance at the top of the atmosphere.

I. INTRODUCTION

Clouds are one of the most important features controlling the radiation budget and climate of the earth. They cover about 50 % of the sky on a global scale (Sasamori, et al.,1972) and significantly modulate solar and infrared radiation on a global scale far more than any other constituents by their reflection and absorption of short wave radiation, and their emission of infrared radiation. In addition, the interaction of radiation with clouds affects cloud development and microphysics.

The primary objectives of this investigation are to develop a theoretical model for the spectral absorption of solar radiation in clouds, and to investigate the dependence of cloud absorption on cloud environmental parameters. The relative contribution of liquid water and water vapor within the cloud is also examined. For the purposes of the present study, the clouds are assumed to be plane-parallel homogeneous media with uniform drop size distribution, and to be embedded in a variety of atmospheric models.

Tropospheric absorption of solar radiation in the absence of cloud takes place mainly in the water vapor absorption bands, ranging from 0.7 μm to 3.5 μm(or from about 2800 to

15000 cm^{-1} in wavenumbers). In the presence of clouds, the absorption and scattering by cloud particles substantially modify the radiation field of the atmosphere over this spectral range. In addition, droplet absorption also occurs outside of water vapor bands.

In calculating the absorption of solar radiation in clouds, one of the major problems is how to incorporate both liquid water absorption and vapor absorption in the presence of multiple scattering by cloud droplets. The task of accurately determining relative absorption by liquid water and water vapor has hitherto remained an unanswered question. Stephens (1978) suggested that the absorptions of solar radiation by liquid water and by water vapor are equally significant. However, Welch and Cox (1980) concluded that droplet absorption is primarily responsible for absorption of solar radiation in thin clouds, and roughly of equal importance to water vapor in thick clouds. According to Slingo and Schrecker (1982), droplet absorption is responsible for the bulk of the total absorption, while water vapor has a only minor contribution.

The amount of water vapor above the cloud regulates total cloud absorption by modifying the amount of incident solar radiation on the top of cloud. Welch, et al. (1976) have suggested that as the cloud top is raised, the increase in available energy in the water vapor absorption bands outweighs decreasing water vapor concentration within the

cloud due to lower temperature, so that total cloud absorption may increase with height.

The model developed here therefore includes the effect of atmospheric water vapor above the cloud, as well as yielding the relative spectral absorption by liquid water and water vapor within the cloud. In addition, seasonal and zonal variations of cloud absorption are estimated by using three different cloud types and five different atmospheric models.

In Chapter II, a number of papers, including both measurements and theoretical studies, are reviewed in a survey of cloud absorption studies. Chapter III discusses the basic theory and fundamental equations used in the development of a spectral model of cloud absorption, including the relative absorption by liquid water and water vapor. Chapter IV presents cloud absorption results for three types of cloud and five different atmospheric models. In addition, spectral cloud absorption and atmospheric water vapor absorption above the cloud is also discussed. Finally, the global application of the model results is briefly discussed.

II. A SURVEY OF CLOUD ABSORPTION STUDIES

Chapter II discusses some of the previous work on cloud absorption, including global cloud absorption, aircraft measurement, and theoretical studies. In addition, some problems involved in the measurement and theoretical calculations are discussed.

2.1 Measurements of Cloud Absorption

Although global cloud coverage is known to be about 50 % of the atmosphere, there are a number of different values of global absorption by clouds. Table 2.1, as an example, compares the values for global cloud absorption suggested by a number of different authors (Liou,1980). It is noted that the values of Houghton and London are for the Northern Hemisphere, and that of Sasamori et al. is only for the Southern Hemisphere. The global absorption by Paltridge and Platt(1976) is based on global and multi-annual averages. As shown in Table 2.1, the wide range of global absorption makes it difficult to evaluate the effect of clouds on global radiation budget. The range of values, from 5 to 37 W/m^2, exceeds the change in the earth's heat budget due to doubling CO_2 content, or to a 2 % change in solar constant,

Table 2.1

Global Absorption and Absorbed Energy by Clouds

	Global Absorption	Absorbed Energy (W/m^2)
Houghton	10	34
London	1.6	5
Sasamori, et al.	4	14
Paltridge and Platt(1976)	11	37
Wittman	4	14

The above values except for Paltridge and Platt are quoted from Liou(1980). The global absorption is expressed as a percentage of the mean insolation at the top of the atmosphere, 340 W/m^2, which is 100 units.

which corresponds to 4-5 W/m^2(Clark,1982).

The extent to which clouds absorb solar radiation is still a question of some debate. Theoretical calculations of fractional absorption do not show general agreement with aircraft measurements of Reynolds, et al.(1975). According to the actual measurements of stratus clouds, the fractional absorption of the incident radiation above the clouds ranges from 0 % to 23 %(Herman,1977). However the mechanism responsible for this large variability has not been clearly explained. The variation may be expected because clouds are affected by dynamical variables associated with transient atmospheric processes and exhibit significant variability on small scales of time and space. Furthermore, measurement errors are invariably present.

2.2 Theoretical Studies of Cloud Absorption

For the accurate calculation of cloud absorption over a given spectral band, we have to consider the problems of multiple scattering of photons between cloud droplets and spectral variation of absorption by liquid water and water vapor. These problems are complicated by the fact that multiple scattering increases the optical path of photons in clouds, and the simple extinction law, Beer's law, applies only to monochromatic radiation. Two methods are commonly used in treating vapor absorption in the presence of multiple scattering. The first method is an exponential sum

fit to the transmission function, in which the broad band transmissivity is approximated by a finite sum of exponentials (Wiscombe and Evans,1977). An alternative technique is the use of photon pathlength distributions, in which a multiple scattering model is used to obtain the probability distribution of photon paths through the clouds. The cloud absorption is then found by integrating the actual spectral transmission function over the pathlength distribution. Although the two methods differ in their approach, Bakan et al.(1978) showed that they are formally equivalent.

A simpler approach was adopted by Lacis and Hansen (1974) who calculated cloud absorption using a k-distribution method to account for water vapor absorption. Their method is somewhat similar to the exponential sum fit of transmission, but introduces a single probability distribution for the absorption coefficients of water vapor.

In a different method from Lacis and Hansen(1974), Krasnokotskaya and Romanova (1974) used a pathlength distribution method to calculate fractional reflection, transmission and absorption by clouds in the water vapor absorption bands. However, they did not point out the relative contribution by water vapor and droplets for each absorption band. They suggested that clouds absorb 6-12 % of solar flux falling on their upper boundary and that this range of values is weakly dependent upon the optical

thickness of the clouds.

Twomey (1974) calculated fractional absorption for clouds with a thickness of 1 km by the doubling method. His values indicate that clouds absorb 8 to 17 % of total incoming solar flux, depending on solar zenith angle and cloud type. However, there is a limitation in Twomey's work because his calculation is restricted to a 1 km thick cloud layer, and is based on exponential absorption by water vapor.

Following Liou (1976), thick clouds such as nimbostratus and cumulonimbus reflect 80-90 % and absorb 10-20 % of the solar radiation incident upon them. For thin stratus clouds whose thickness is 0.1 km, the reflection is about 45-72 % and the absorption is about 1-6 % of the solar flux incident on the cloud. His theoretical calculation suggested that maximum cloud absorption does not exceed 20 % of the incident radiation on the cloud top.

By the method of exponential sum fitting of transmission, Stephens (1978) calculated cloud absorption. His conclusion is that the absorption of solar radiation by droplet and by water vapor in clouds is equally significant. He also suggested that the fractional absorption is almost independent of height after allowing for absorption by water vapor above the cloud.

Welch, et al. (1976) showed that droplet absorption in the 2.7 and 3.3 μm water vapor bands has a significant

contribution to cloud heating rates. Using a spherical harmonics technique, Welch and Cox (1980) examined the relative absorption by water vapor in cloud absorption and its contribution to heating rates. According to their results, water vapor contributes approximately 20 % of cloud heating near the cloud top, but up to 50 % of cloud heating averaged over cloud thickness of 1 km.

From a study on the shortwave radiative properties of stratiform clouds, Slingo and Schrecker (1982) concluded that droplets are responsible for the bulk of the absorption, and water vapor makes a minor contribution to total cloud absorption.

As discussed in this section, estimation of the relative absorption of liquid water and water vapor in cloud has been quite variable, depending on the authors, and it is difficult to assess the range of cloud absorption and relative absorption by liquid water and water vapor within cloud. These inconsistent conclusions may be due to the lack of detailed spectral models which include the accurate scattering and transmission of solar radiation within cloud. However, the main reason for this lack appears to be the computational effort required to account for both multiple scattering effects, as well as detailed spectral transmission in water vapor.

The present study attempts to estimate accurately the relative absorption of liquid water and water vapor in clouds. The calculations are performed by using a spectral model which takes into account the effects of multiple scattering and spectral absorption of water vapor in clouds.

III. THEORY

In this chapter a brief discussion of optical parameters, including drop size distribution and water vapor density is presented. In addition, the basic equations for the calculation of cloud absorption and computational procedure are also developed.

3.1 Physical Parameters Related to Cloud Absorption

Usually, a cloud is defined as a visible aggregate of very small droplets, ice crystals, or a mixture of both, with its base above the earth's surface. However, for a more detailed description of the physical characteristics of a cloud, it is necessary to introduce other physical parameters such as; (1) shape, (2) dimensions, (3) three dimensional drop and ice crystal size distributions, (4) temperature distribution, (5) cloud height from the earth's surface, and (6) relative volume of ice crystals and liquid water. The amount of radiant energy which is reflected and absorbed by a cloud is closely related to all of these factors. In addition, cloud absorption also depends on a few other factors, such as, surface albedo, solar zenith angle, atmospheric water vapor content, and presence of

other cloud layer(s). Among the previous factors, the drop size distribution and water vapor content are the most important factors, and will be discussed in this section.

3.1.1 Drop Size Distribution

The number density of cloud drops and range of drop sizes vary significantly in nature. They are not only highly dependent upon cloud type, but also on cloud height, geometrical thickness, season, and geographical position.

In the present study, clouds are assumed to be plane-parallel media which have a homogeneous liquid drop size distribution and a uniform water vapor density in saturation. This assumption allows the use of a simplified cloud model. For the parameterization of drop size distribution, the modified gamma distribution which was derived from experimental data is used (Tampier and Tomasi,1976). This distribution function gives the number density of droplets per unit radius as a function of radius in the form of

$$N(r) = \alpha r^{\delta} \exp\left[-\frac{\delta}{\gamma}\left(\frac{r}{R}\right)^{\gamma}\right] \qquad (3.1)$$

where α, δ and γ are empirically derived constants, based on the experimental drop size distribution. The parameter R refers to the modal radius. Table 3.1 (Welch and Cox,1980) gives the parameters for the three clouds used in this

Table 3.1

Cloud Drop Size Distribution Parameters

Cloud Type	α	δ	γ	R (μm)	LWC (g/m^3)	N_0 (cm^{-3})
Stratocumulus (base)	.2823	5	1.19	5.33	0.141	100
Nimbostratus (top)	1.0969	1	2.41	9.67	1.034	100
Stratus(top)	.3818	3	1.30	6.75	0.379	100

Note; LWC: liquid water content, N_0: number density of droplet.

study. The three parameters except for α completely determine the shape of the distribution curve while the constant α is only related to the total number of droplets per unit volume.

3.1.2 Water Vapor Content

Water vapor amount within cloud is determined assuming 100 % relative humidity. The saturated water vapor density (g/m^3) is obtained from the empirical formula used in LOWTRAN 5 (Kneizys, et al., 1980), given by

$$\rho(t) = A \exp(18.9766 - 14.9595A - 2.4388A^2) \qquad (3.2)$$

where A=273.15/(273.15+t), and t is the mean temperature of a cloud in °C. This equation is a good approximation of saturated water vapor density for the temperature ranging from - 50 °C to + 50 °C.

Since the half width and effective strength of an absorption line are dependent upon pressure and temperature, the water vapor density must first be scaled to standard pressure and temperature before being used in the calculation of water vapor absorption. The scaled water vapor density $\rho^*(t)$ is obtained through equation (3.3)

$$\rho^*(t) = \rho(t)\left(\frac{\bar{P}}{P_0}\right)\left(\frac{T_0}{\bar{T}}\right)^{\frac{1}{2}} \qquad (3.3)$$

where $\bar{P}$ and $\bar{T}$ indicate the mean pressure and temperature of

a cloud layer. P_0 and T_0 correspond to STP(1013 mb, 273 K).

For the computation of atmospheric vapor absorption above the cloud, the effective water vapor amount is obtained by integrating the specific humidity q with respect to pressure, scaling as in equation (3.3). That is

$$y = \frac{1}{g_0} \int_0^{P_t} q \left(\frac{\bar{P}}{P_0}\right)\left(\frac{T_0}{\bar{T}}\right)^{\frac{1}{2}} dp \qquad (3.4)$$

where P_t is the pressure at the cloud top. g_0 is the gravitational acceleration of the earth. Actually, y corresponds to the effective water vapor amount above the cloud, and is given in cm. This value of y may then be used to calculate atmospheric vapor absorption using LOWTRAN 5.

In the present work, five different atmospheric models (McClatchey et al.,1972; Welch and Cox,1980) are used for the calculation of water vapor amounts above the cloud. The mean temperature and pressure of a cloud are also determined from these models.

3.1.3 Cloud Size

The shape, size, and thickness of cloud may be considered as continuous variables. They are dependent on season, geography, and atmospheric state. For the calculation of cloud absorption, a homogeneous plane-parallel cloud is assumed. The extent of the cloud is infinite in the horizontal direction. The cloud thickness is assumed to be

1 km as a reference thickness for the calculation of cloud absorption. This is consistent with the typical thickness of cumulus cloud (Paltridge and Platt,1976).

3.2 Optical Parameters of Cloud Droplets from Mie theory

Mie theory (Zdunkowski and Strand,1969; McCartney,1976, Van de Hulst,1981) has been known to give a nearly complete solution to the problem of scattering and absorption by an isolated sphere. The theory is based on the assumption that the particle is a homogeneous sphere with a sharp discontinuity of refractive index at its surface.

The extinction by a spherical particle is described in terms of its size parameter and its complex refractive index. The size parameter X is defined as the ratio of the particle radius r to wavelength λ, ie,

$$X = \frac{2\pi r}{\lambda} \tag{3.5}$$

To include the effect of absorption, the refractive index of the medium may be expressed as a complex number. In this case, the index of refraction is represented by

$$\eta(\lambda) = \eta_r(\lambda) - i\,\eta_i(\lambda) \tag{3.6}$$

Here $n_r(\lambda)$ and $n_i(\lambda)$ stand for the real and imaginary indices of refraction, respectively.

Using the size parameter for a single droplet and the complex refractive index for pure water, the extinction efficiency factor $Q_{ex}(x,\lambda)$, scattering efficiency factor $Q_{sc}(x,\lambda)$, and asymmetry factor $g(x,\lambda)$ may be obtained using Mie theory. Wiscombe's computer code(1979) was used for this purpose together with data on refractive indices of water from Irvine and Pollack(1968) and Hale and Querry(1973). For a cloud made up of spherical droplets with drop size distribution N(r),the volume extinction coefficient, is then found by integrating over size distribution as

$$\beta_{sc}(\lambda) = \int_0^\infty \pi r^2 N(r) Q_{sc}(\lambda, r)\, dr \tag{3.7}$$

Similarly, the volume absorption coefficient $\beta_{ab}(\lambda)$ or the volume extinction coefficient $\beta_{ex}(\lambda)$ may be calculated by replacing the Mie scattering efficiency factor by the Mie efficiency factor for absorption, $Q_{ab}(\lambda,r)$, or extinction, $Q_{ex}(\lambda,r)$.

The single scattering albedo $\omega(\lambda)$ is defined as the ratio of scattering to extinction,

$$\omega(\lambda) = \frac{\beta_{sc}(\lambda)}{\beta_{sc}(\lambda) + \beta_{ab}(\lambda)} \tag{3.8}$$

The angular distribution of scattered radiation by an element of volume, including polarization, may be determined

explicitly using the Mie phase matrix. In the present study, it is assumed that the transfer of radiation within cloud is dominated by multiple scattering so that polarization effects are negligible. This situation allows the use of the Mie phase function $P(\theta)$, which is normalized such that

$$\frac{1}{4\pi}\int_{4\pi} P(\theta)\, d\Omega = 1 \tag{3.9}$$

where θ is the scattering angle and $d\Omega$ is the solid angle.

The effects of multiple scattering may be further summarized by the asymmetry factor, $g(\lambda,r)$, defined as the solid angle average of $\cos\theta$ weighted by the phase function

$$g(\lambda,r) = \frac{1}{2}\int_{-1}^{+1} P(\theta,\lambda,r)\cos\theta\, d(\cos\theta) \tag{3.10}$$

The asymmetry factor for a distribution of droplet sizes is found by integrating the individual asymmetry values as:

$$g(\lambda) = \frac{\int_0^\infty \pi r^2 N(r) Q_{sc}(\lambda,r)\, g'(\lambda,r)\, dr}{\int_0^\infty \pi r^2 N(r) Q_{sc}(\lambda,r)\, dr} \tag{3.11}$$

where $g'(\lambda,r)$ is the asymmetry factor for a single droplet.

3.3 Results for Spectral Values of the Cloud Parameters

Figure 3.1 illustrates the asymmetry factor, optical thickness of scattering, and single scattering albedo as a function of wavenumber for the stratocumulus and nimbostratus clouds specified in Table 3.1. The spectral dependence of g , τ_s and ω for stratus cloud is omitted from Figure 3.1 for clarity as they were found to be intermediate between the nimbostratus and stratocumulus values. The curves of g and τ_s do not show a large variation except in the vicinity of the strong absorption band at about 3000 cm^{-1}. For example, the value of τ_s for a nimbostratus cloud ranges from about 52 to 103, and the value of asymmetry factor from 0.84 to 0.98. Apart from this variation, the values of g and τ_s are nearly constant, and remain about 0.86 and 100 elsewhere. For stratocumulus cloud, the value of g is between 0.77 and 0.97. The value of τ_s ranges from 14 to about 34. The highest variations of g and τ_s are again restricted to the spectral region between about 2000 cm^{-1} and 4000 cm^{-1}. Excluding the region of high variation, the values of g and τ_s are about 0.86 and 28, respectively.

Figure 3.1 is a plotting of $\log(1-\omega)^{-1}$ against wavenumber. The values of single scattering albedo, ω, in Figure 3.1 increase with wavenumber, showing some oscillations. The value of $\log(1-\omega)^{-1}$ changes from about 0.3 to 5.5. However, the value of $\log(1-\omega)^{-1}$ does not show large differences for the three different cloud types.

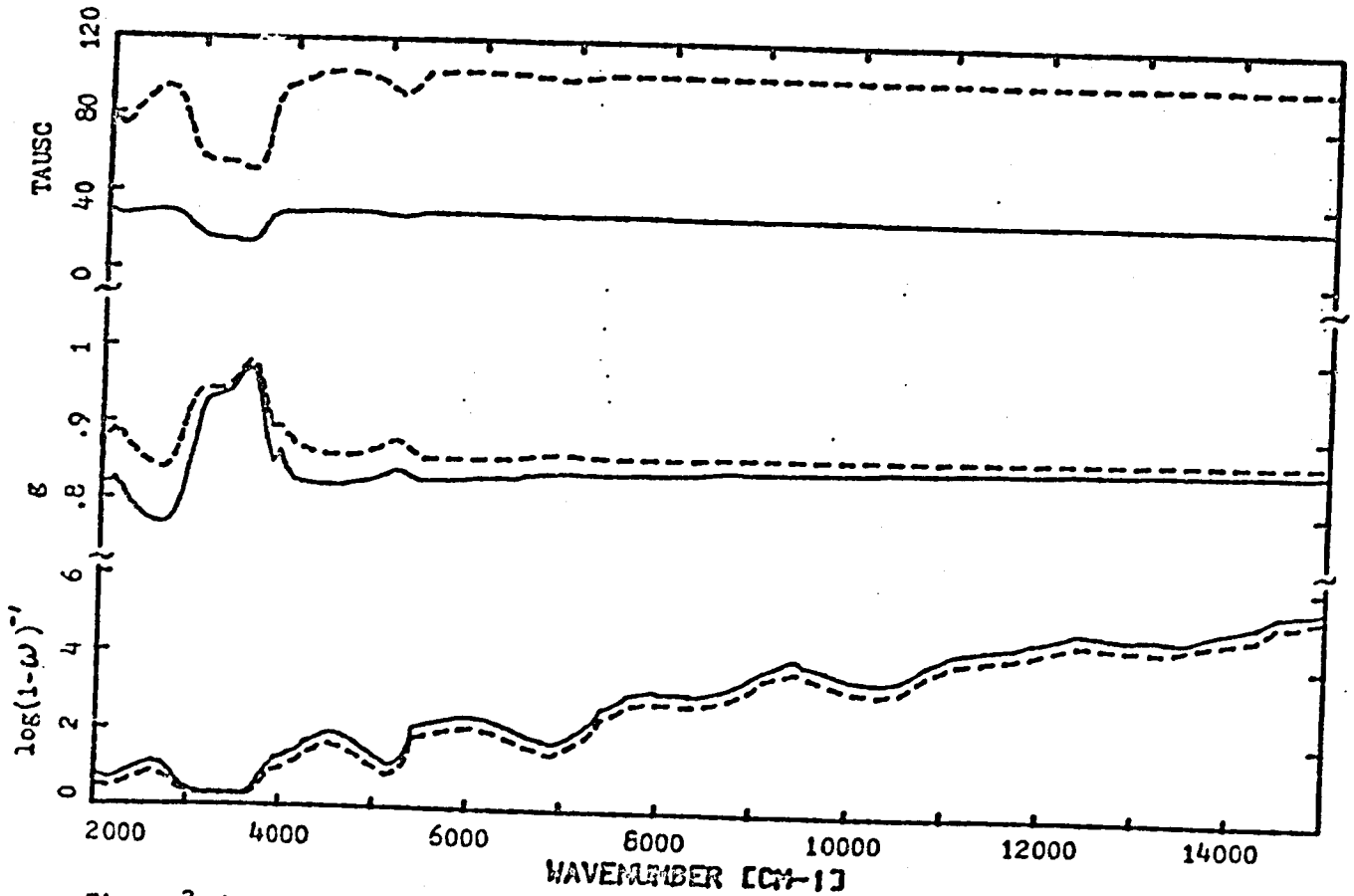

Figure 3.1 Asymmetry factor(g), scattering optical thickness(τ_{sc}), and single scattering albedo(ω) as a function of wavenumber.

The dashed and solid lines present nimbostratus and stratocumulus clouds, respectively.

Among the optical parameters of cloud droplets, the scattering optical thickness and asymmetry factor are used to generate photon pathlength distribution of upward and downward flux under conservative scattering. The values of τ_c and g are selected approximately, based on calculations. For the calculation of pathlength distributions, the value of g is fixed at 0.86 for the three types of cloud because it does not show as much variation as the value of the scattering optical thickness which was normally chosen as 28 for stratocumulus, 54 for stratus cloud and 100 for nimbostratus, corresponding to clouds of ~1 km thickness. The variations of g and τ_c around 3000 cm^{-1} may be neglected because absorption dominates scattering in this small spectral region.

3.4 Photon Pathlength Distribution

The incident solar radiation is absorbed and scattered within a cloud layer by the interaction of photons with the cloud droplets. For a moderately dense cloud, the direct solar beam rapidly loses its identity as a result of multiple scattering. Therefore, the amount of absorption and scattering is highly dependent upon the pathlength traveled by a beam of radiation rather than directly on the geometrical thickness of the cloud.

The notion of the pathlength distribution dates back to Fock's paper in 1926(Van de Hulst,1980),and is applicable to

the cloud with multiple scattering (Irvine,1964 and 1963; Danielson et al.,1969; Appleby and Irvine, 1973;Bakan and Quenzel,1976).

When solar radiation is scattered in the cloud, the scattered radiation leaving the cloud is composed of photons with different paths. The pathlength distribution, $P(\ell)$ is defined to be the probability per unit pathlength that photons will travel a distance ℓ before emerging from the cloud. The pathlength distribution, $P(\ell)$ is normalized over all possible pathlengths such that

$$\int_0^\infty P(\ell)\,d\ell = 1 \qquad (3.12)$$

The pathlength distribution has been obtained from a Monte Carlo simulation of the actual process of photon transmission through a cloud layer with conservative scattering, using the model of Davies(1978). The model was run for specified g , τ_c and solar zenith angle, θ_0, with 10^5 simulations per case.

Figure 3.2 shows an example of the photon pathlength distribution of scattering radiation in the case where $\theta_0=0^\circ$, $g=0.86$, and $\tau_c=100$. The pathlength distribution, $P(\ell)$ decreases asymptotically for large pathlength, and has a maximum value at about 0.1 km. This peak is due to the reflected photons from the cloud layer. The figure is truncated at 2 km, beyond which $P(\ell)$ continues to decrease

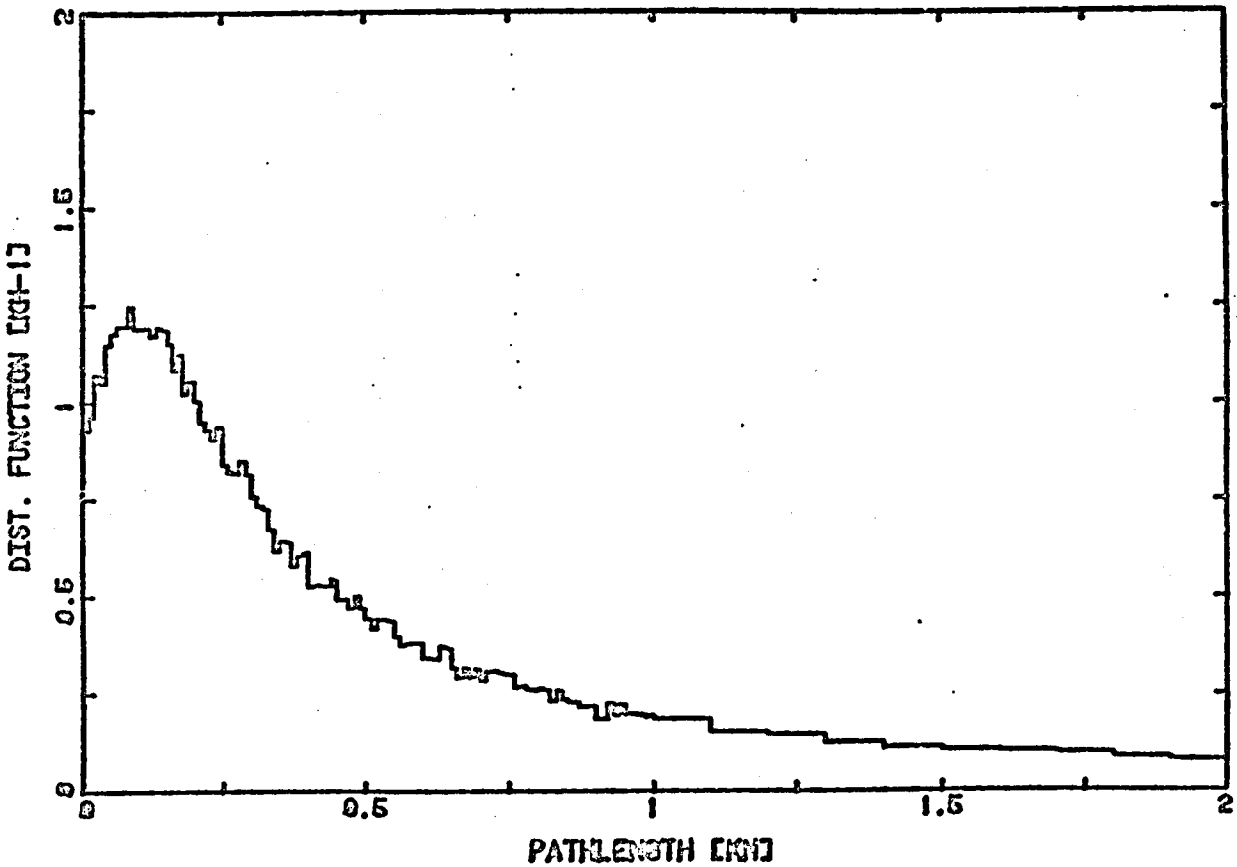

Figure 3.2 Photon pathlength distribution as a function of pathlength for nimbostratus cloud.

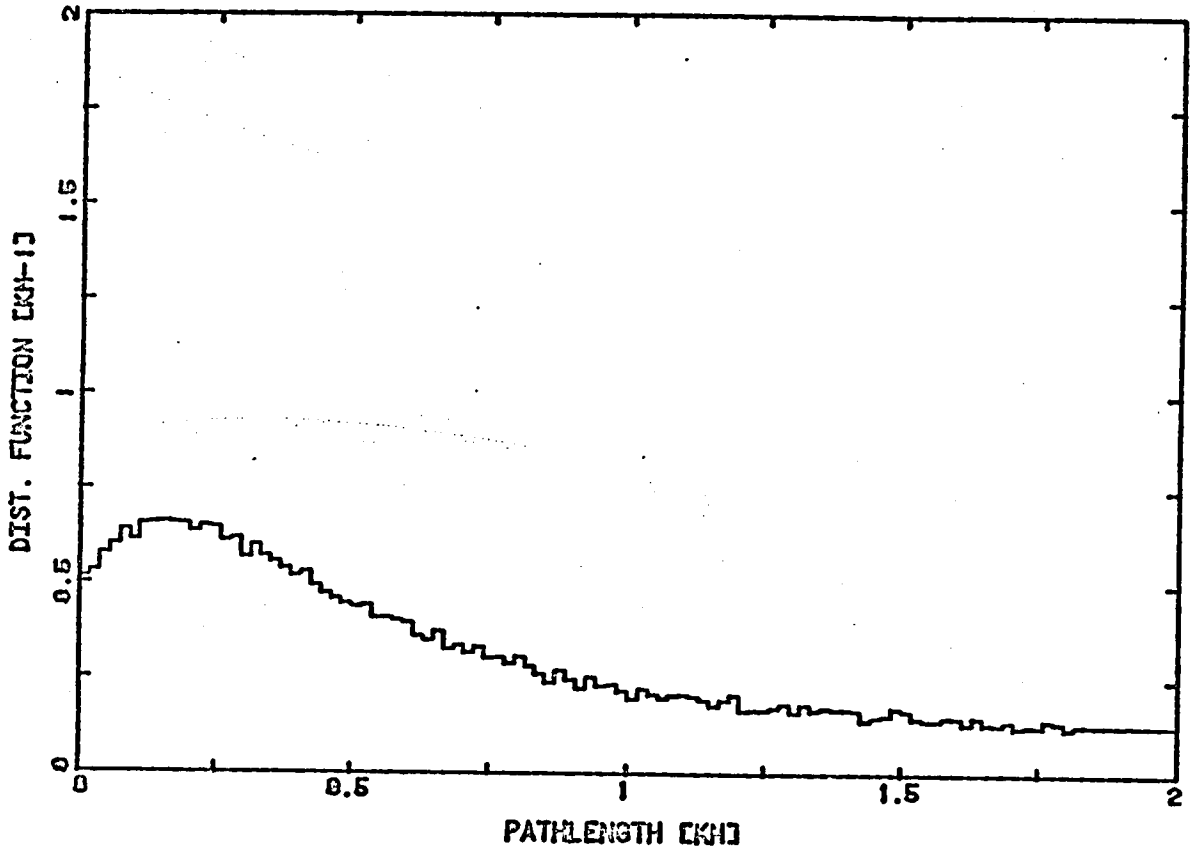

Figure 3.3 Photon pathlength distribution as a function of pathlength for stratus cloud

The distribution function is obtained under the conditions; $\theta_0 = 0$, $\vartheta = 86$, and $\tau_c = 54$.

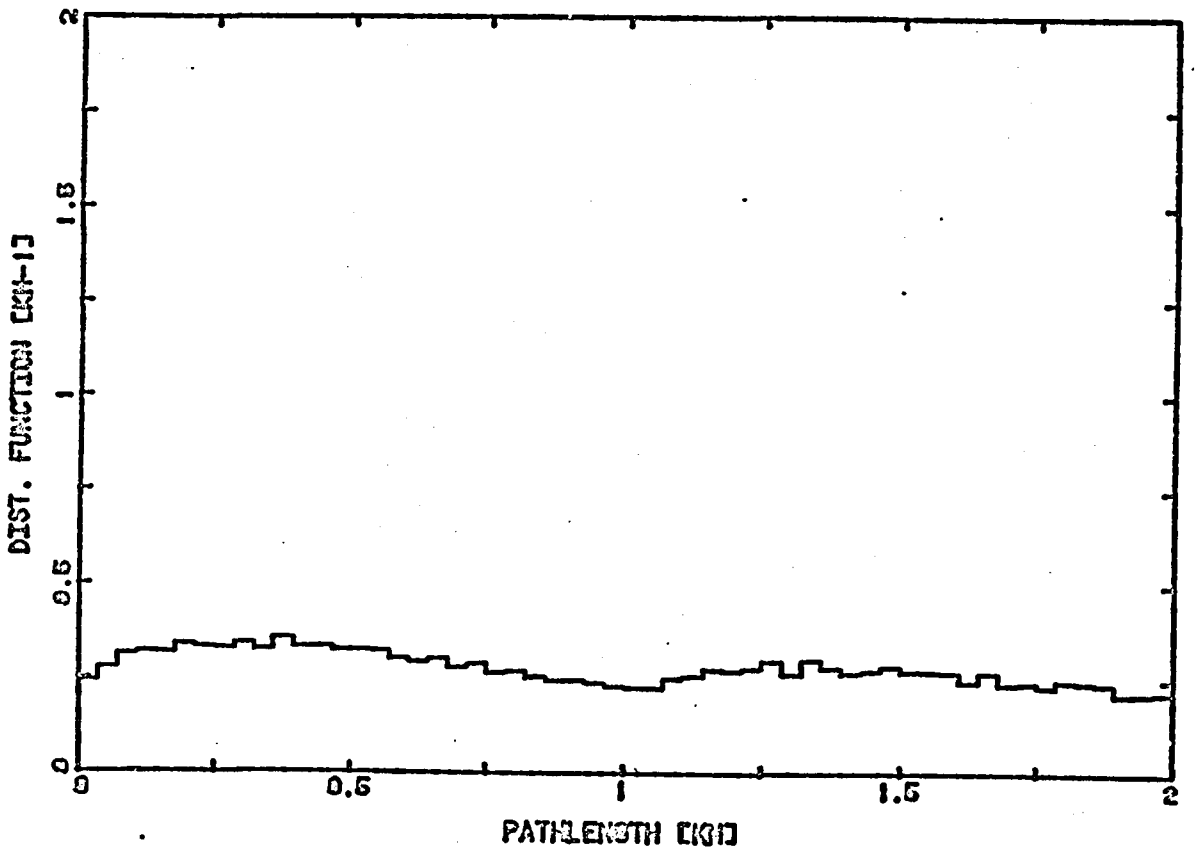

Figure 3.4 Photon pathlength distribution as a function of pathlength for stratocumulus cloud.

The distribution function is obtained under the conditions; $R = 0$, $g = 0.86$, and $\tau_c = 28$.

asymptotically. Figure 3.3 illustrates the typical photon pathlength distribution for a stratus cloud. The pathlength which corresponds to the maximum value of $P(\ell)$ is slightly larger than that of $P(\ell)$ in Fig. 3.2. The maximum value of $P(\ell)$ in Figure 3.3 is about a half of the $P(\ell)$ in Figure 3.2. The decrease of maximum value of $P(\ell)$ is due to the decrease of the scattering optical thickness. The value of $P(\ell)$ after 0.5 km is higher than that of $P(\ell)$ in Figure 3.2. This higher value may be explained by the higher transmission due to lower scattering optical thickness.

The pathlength distribution of stratocumulus clouds is displayed in Figure 3.4. The primary peak at about 0.25 km is due to the reflected photons while the secondary peak at about 1.25 km is due to the transmitted photons. As can be seen in Figure 3.4, the transmitted photons are equally significant to the reflected photons for a given pathlength. A comparison of these three figures shows that as τ_{sc} decreases, the value of $P(\ell)$ for reflected photons decreases while the value of $P(\ell)$ for transmitted photons increases.

3.5 Transmission Function of Cloud

Figure 3.5 presents an example of water vapor transmission, at 20 cm^{-1} resolution obtained from LOWTRAN 5, and shows the very rapid change of water vapor transmission with wavenumber. This figure clearly illustrates a higher

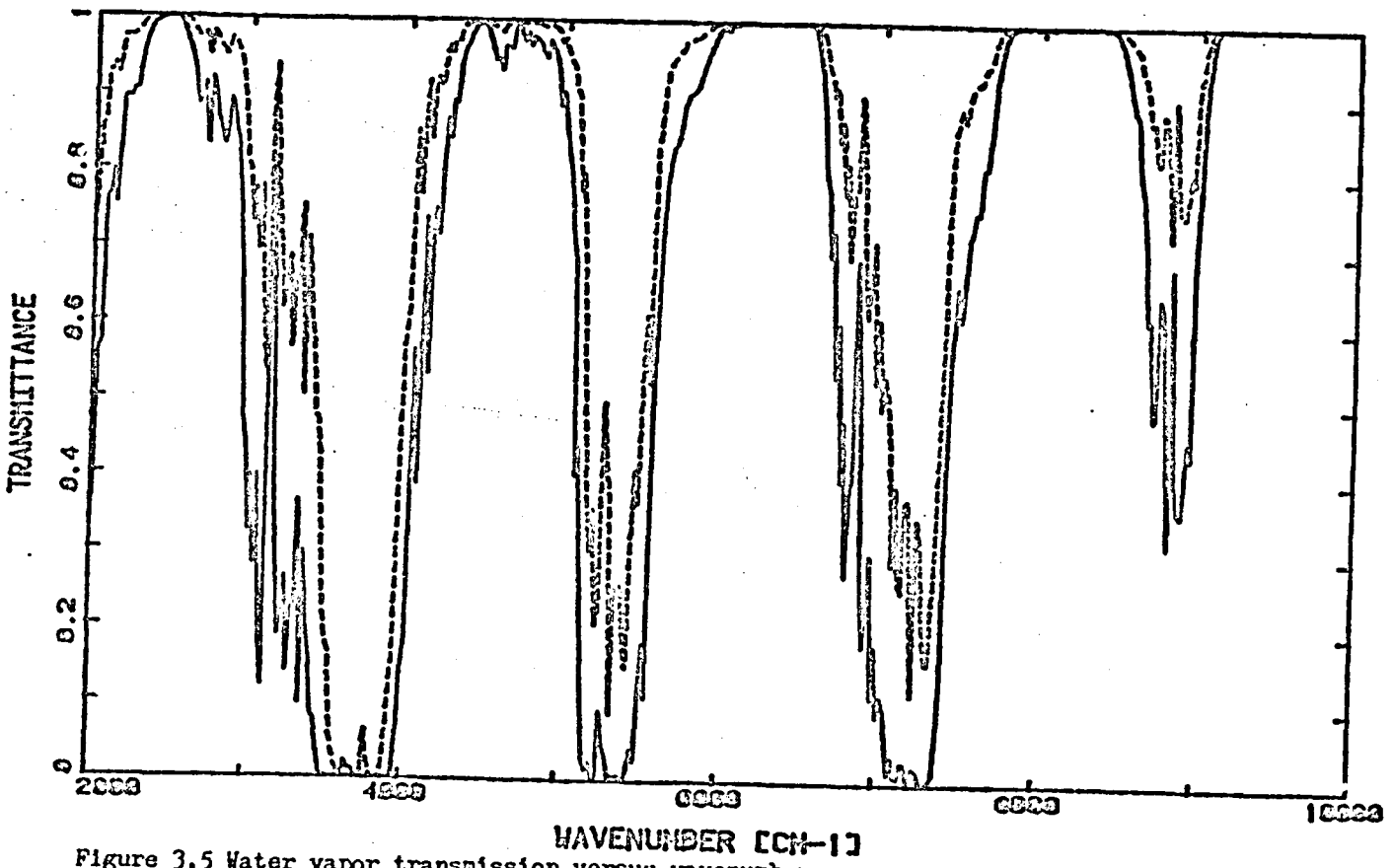

Figure 3.5 Water vapor transmission versus wavenumber.
The dashed and solid lines represent transmittance for equivalent water vapor paths of 0.1 and 1 cm, respectively. The figure is obtained from LOWTRAN 5(Kneizys et al.,1980).

transmission for a smaller value of the equivalent water vapor path. For a finite spectral interval $\Delta\nu_i$, the water vapor average transmission function may be expresed as

$$\bar{T}'_{\Delta\nu_i}(\ell) = \frac{1}{\Delta\nu_i}\int_{\Delta\nu_i} e^{-\beta'(\nu)\ell}\, d\nu \tag{3.13}$$

where $\beta'(\nu)$ is the volume absorption coefficient of water vapor, and ℓ is photon pathlength. It is noted that in equation (3.13), $\bar{T}'_{\Delta\nu_i}(\ell)$ will no longer necessarily vary exponentially with ℓ due to the rapid spectral variability of $\beta'(\nu)$.

In the case of a homogeneous cloud composed of water vapor and liquid water, the cloud transmission function can be obtained by combining liquid water and water vapor transmission functions. The cloud transmission function can be written as;

$$\bar{T}_{\Delta\nu_i}(\ell)_{CD} = \left[\bar{T}^*_{\Delta\nu_i}(\ell)\right]\left[\bar{T}'_{\Delta\nu_i}(\ell)\right] \tag{3.14}$$

where the subscript CD means cloud, and $\bar{T}^*_{\Delta\nu_i}(\ell)$ is the transmission function of liquid water. The transmission function of liquid water is given in the form of

$$\bar{T}^*_{\Delta\nu_i}(\ell) = \frac{1}{\Delta\nu_i}\int_{\Delta\nu_i} e^{-\beta(\nu)\ell}\, d\nu \tag{3.15}$$

where $\beta(\nu)$ is the volume absorption coefficient of liquid

water. The spectral interval, $\Delta\nu_i$ in equation (3.15) should be chosen small enough so that the droplet scattering properties and $\beta(\nu)$ remain relatively constant.

3.6 Spectral Cloud Absorption

To include the effect of water vapor absorption above the cloud, the composite transmission function for photons with pathlength ℓ within the cloud may be written as;

$$\bar{T}_{\Delta\nu_i}(\ell, y_c)_{cD} = \left[\bar{T}^{*}_{\Delta\nu_i}(\ell)\right]\left[\bar{T}'_{\Delta\nu_i}(y_c, y(\ell))\right] \qquad (3.16)$$

The quantities y_c and y in the equation (3.16) are the equivalent water vapor amount from the top of atmosphere to cloud top and the water vapor amount in cloud, respectively. The values of y and y_c are obtained through the equations (3.3) and (3.4). Using the cloud transmission function and pathlength distribution, the cloud absorption, $A(\mu_0)_{\Delta\nu}$ for a given $\Delta\nu$ is obtained from

$$A(\mu_0)_{\Delta\nu} = \int_{\nu_1}^{\nu_2} F_\nu(\mu_0) \int_0^\infty P_\nu(\mu_0, \ell)\left[\bar{T}'_{\Delta\nu_i}(y_c) - \bar{T}_{\Delta\nu_i}(y_c, \ell)_{cD}\right] d\ell\, d\nu \qquad (3.17)$$

where $\mu_0 = \cos\theta_0$ and $\Delta\nu = \nu_2 - \nu_1$. $\Delta\nu_i$ is the subdivision of $\Delta\nu$ and the value of $\Delta\nu_i$ is assigned as 20 cm^{-1} in the actual calculation. F_ν represents spectral solar irradiance at the top of the atmosphere. The values of solar spectral irradiance are taken from Thekaekara and Drummond(1971).

To determine relative absorption, we need the two separate equations for the two absorbing constituents of the cloud. The liquid water absorption, $\hat{A}(\mu_0)_{\Delta\nu}$ is calculated through

$$A^{*}(\mu_0)_{\Delta\nu} = \int_{\nu_1}^{\nu_2} F_{\nu}(\mu_0) \int_{0}^{\infty} P_{\nu}(\mu_0, \ell) \left[\int_{0}^{\ell} \bar{T}'_{\Delta\nu_i}(y_0, y(\ell')) \cdot \left(\frac{-d\bar{T}^{*}_{\Delta\nu_i}(\ell')}{d\ell'} \right) d\ell' \right] d\ell \, d\nu \qquad (3.18)$$

Similarly, the cloud water vapor absorption is given in the form of

$$A'(\mu_0)_{\Delta\nu} = \int_{\nu_1}^{\nu_2} F_{\nu}(\mu_0) \int_{0}^{\infty} P_{\nu}(\mu_0, \ell) \left[\int_{0}^{\ell} \bar{T}^{*}_{\Delta\nu_i}(\ell') \cdot \left(\frac{-d\bar{T}'_{\Delta\nu_i}(y_0, y(\ell'))}{d\ell'} \right) d\ell' \right] d\ell \, d\nu \qquad (3.19)$$

In (3.17), (3.18) and (3.19), the spectral pathlength distribution, $P_{\nu}(\ell)$ is not strongly dependent on wavenumber. Therefore, $P(\ell)$ is used instead of $P_{\nu}(\ell)$.

By representing the integrals in the equations (3.17) to (3.19) as finite sums, we obtain the total cloud absorption, droplet absorption, and water vapor absorption. For the numerical integration, the trapezoidal method is used, and all values between data points are linearly interpolated within the possible range of linearity. The values of step size for wavenumber integration and pathlength integration are taken as 100 cm^{-1} and 0.1 km, respectively.

The value of $\Delta\nu_i$ in the water vapor transmission function is chosen as 20 cm^{-1}. The spectral resolution of droplet absorption and scattering, and solar irradiance depends on the degree of variation of volume absorption coefficient, and scattering coefficient, and spectral solar irradiance with wavenumber. The average value of spectral resolution of droplet absorption and scattering coefficient are about 320 cm^{-1} for the interval of integration. The spectral resolution of solar irradiance is about 240 cm^{-1}. Both are consistent with integration steps of 100 cm^{-1}.

3.7 Summary of Cloud Absorption Model

The numerical integration of $A(\mu_0)_{\Delta\omega}$, $\hat{A}(\mu_0)_{\Delta\omega}$ and $\acute{A}(\mu_0)_{\Delta\omega}$ requires a number of input variables: (1) atmospheric model, (2) cloud type, (3) wavenumber interval and step size for numerical integration, (4) solar zenith angle, and (5) altitudes of cloud top and base. For the given cloud type, solar zenith angle, and wavenumber interval for integration, the data for pathlength distribution, volume absorption coefficient of liquid water and spectral solar irradiance are arranged for the calculation of cloud absorption through a main program and subroutine programs. In addition, water vapor transmission is provided from LOWTRAN 5.

It is noted that the volume scattering coefficient of liquid water changes with cloud type, and thus pathlength

distribution is also dependent upon the type of cloud and solar zenith angle. Therefore, the first step in the application of the present model to a different cloud type is to calculate the optical parameters of the cloud using Mie theory. Secondly, the photon pathlength distribution for fixed solar zenith angle should be generated based on the average values of scattering optical thickness and asymmetry factor of the cloud. The calculation of cloud absorption for different solar zenith angles again requires generation of the photon pathlength distribution. The generation of photon pathlength distribution is a major task in the model because it is obtained through the Monte Carlo method and requires a lot of computer time for the simulation of physical processes within a cloud.

The cloud absorptions with changes of cloud top altitude, cloud thickness, and atmospheric model can be obtained directly from the model by assigning the altitudes of cloud base and top, and atmospheric model. The atmospheric model determines the mean temperature and pressure of cloud layer, as well as water vapor amount above the cloud, based on the altitudes of cloud top and base.

The present model can be extended for further application by introducing variations of cloud type and atmospheric model. In addition, the use of pathlength distributions for finite clouds improve the usefulness of this model.

IV. MODEL RESULTS

This chapter presents results from the cloud absorption model for three types of clouds and five different atmospheric models. In the calculation of cloud absorption, the effect of solar zenith angle, cloud thickness, season, and water vapor absorption above the cloud are examined. In addition, a comparison against previously published results has been made to test the present model.

4.1 Spectral Absorption by Water Vapor and Liquid Water

For the investigation of spectral variation of absorption in stratus cloud whose thickness is 1 km, the cloud is assumed to be embedded in an atmospheric model for mid-latitude summer with overhead sun. Figure 4.1 shows the model results for spectral cloud absorption and atmospheric water vapor absorption expressed as fractions of the incident solar irradiance at the top of the atmosphere. As illustrated in Figure 4.1, there are eight and seven dominant spectral bands in the profiles of atmospheric water vapor absorption and cloud absorption, respectively. There are four regions of minimum cloud absorption between 1500 cm^{-1} and 8000 cm^{-1}. These regions are mainly due to the nearly complete absorption by atmospheric water vapor above

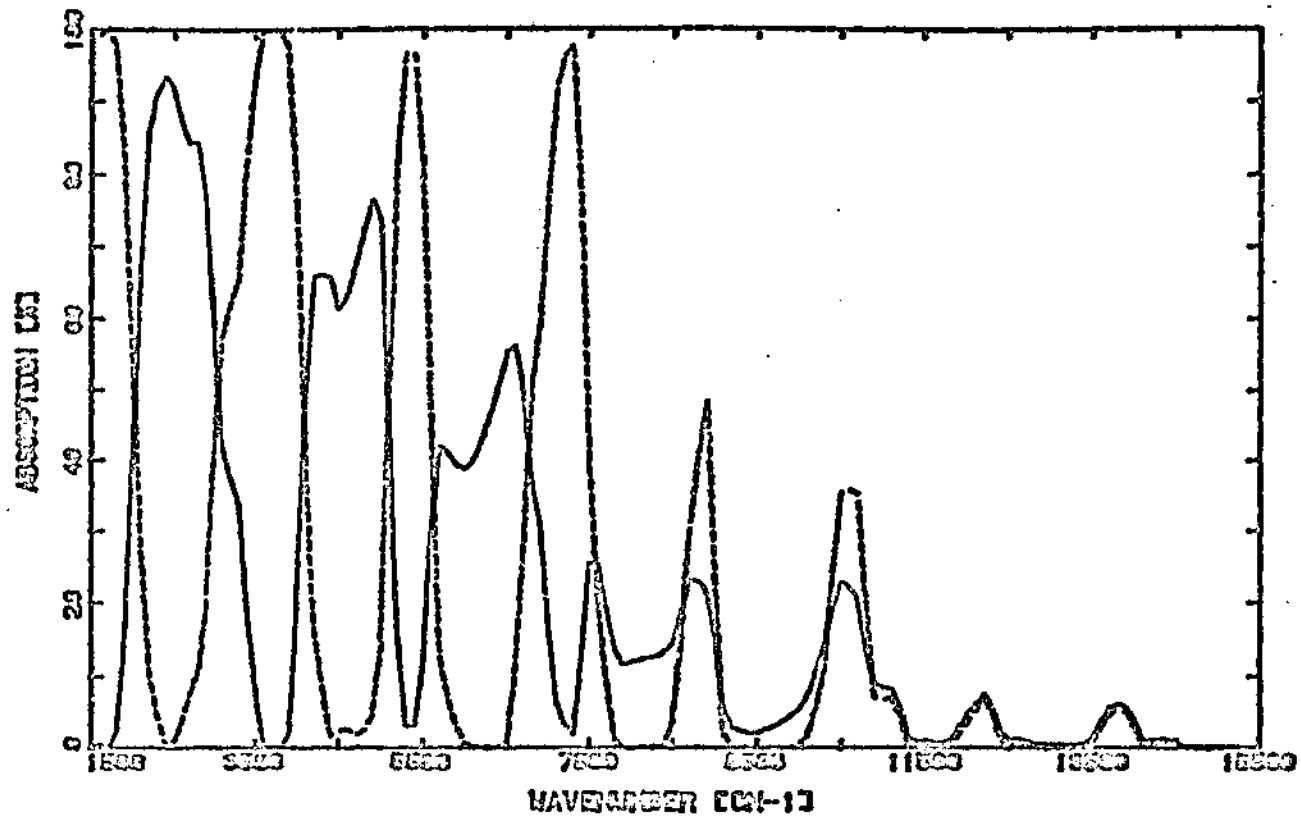

Figure 4.1 Fractional cloud absorption(solid) and atmospheric water vapor absorption (dashed) as a function of wavenumber.

The cloud top altitude is 2 km, and the solar zenith angle is zero.

the cloud. Over this spectral range, there is a general correspondence between the maximum cloud absorption and the minimum atmospheric vapor absorption. The maximum cloud absorption at the point of minimum atmospheric water vapor absorption is due to liquid water absorption, as can be seen in Figure 4.3.

In the spectral region of 8000 to 15000 cm^{-1} in Figure 4.1, the peaks of atmospheric water vapor absorption are superimposed on the peaks of cloud absorption, and their values do not exceed 50 %. This means that the water vapor absorption bands within 8000 to 15000 cm^{-1} are not as strong as the water vapor absorption bands within 1500 to 8000 cm^{-1}. Therefore, some cloud water vapor absorption can be expected because of incomplete absorption by water vapor above the cloud.

Figure 4.2 displays the spectral energy absorbed by cloud and atmospheric water vapor above the cloud as a function of wavenumber. Instead of fractional cloud absorption in Figure 4.1, Figure 4.2 clearly shows the relative contribution of each band to total cloud absorption. A comparison of Figs. 4.1 and 4.2 shows that there is good agreement between the patterns of the curves. However, the maximum fractional cloud absorption and atmospheric water vapor absorption occurs for different wavenumbers than the maximum values of absorbed energy due to weighting by the solar spectrum. In terms of absorbed energy, the maximum

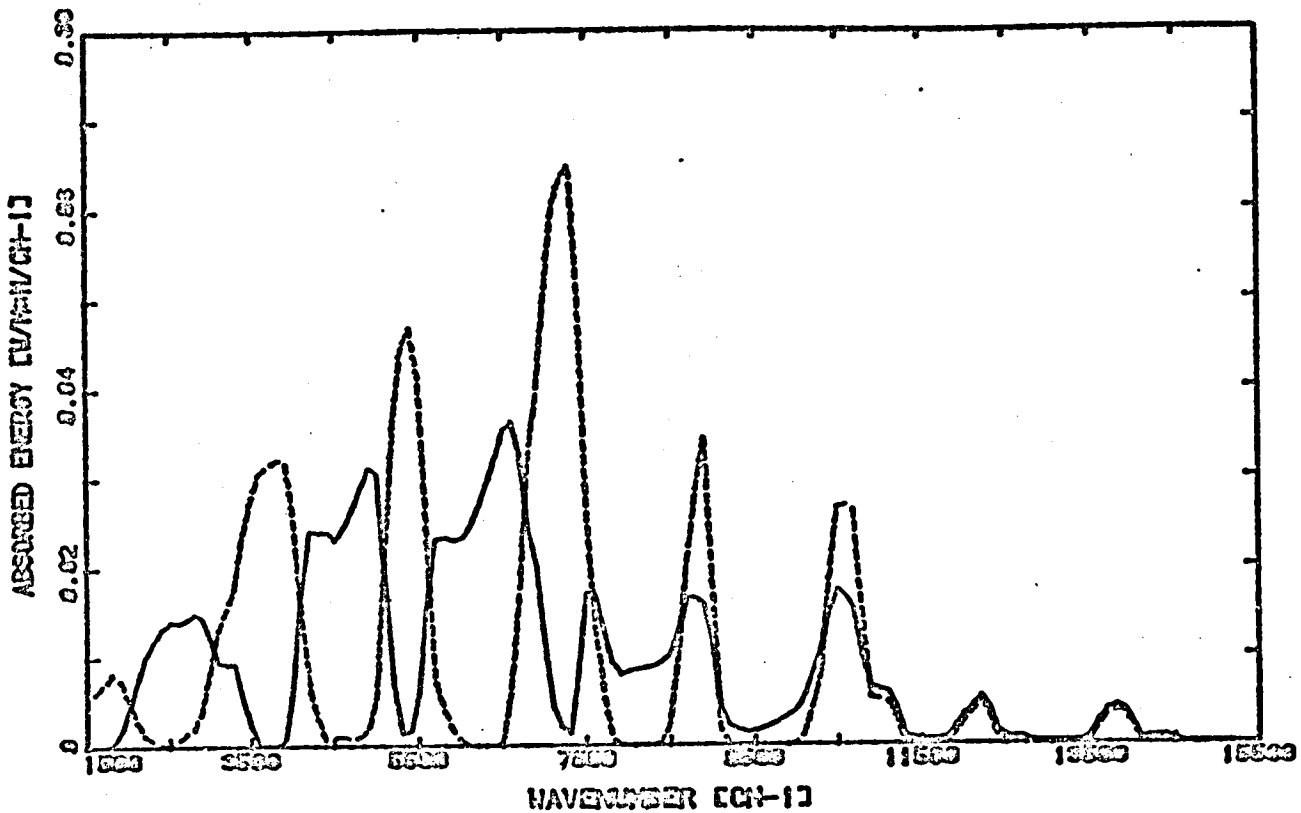

Figure 4.2 Spectral cloud absorption(solid) and atmospheric water vapor absorption above the cloud(dashed).

The same conditions in Fig. 4.1 are used.

cloud absorption occurs between 5500 cm^{-1} and 7000 cm^{-1} while the maximum atmospheric water vapor absorption takes place in the range of 6000 cm^{-1} to 8000 cm^{-1}. Two dominant cloud absorption bands between 4000 cm^{-1} and 7000 cm^{-1} contribute significantly to total cloud absorbed energy. Three absorption bands between 1500 cm^{-1} and 7500 cm^{-1} are the major components of the atmospheric water vapor absorption above the cloud. Over the spectral region of 11500 cm^{-1} to 15000 cm^{-1}, there are two weak bands of cloud and atmospheric water vapor absorption. Almost all the cloud absorption is due to the liquid water absorption between 1500 cm^{-1} and 7500 cm^{-1}, and to water vapor between 11000 cm^{-1} and 15000 cm^{-1}.

Figures 4.3 and 4.4 show the relative contributions to total cloud absorption made by liquid water absorption and absorption by water vapor within the cloud. As can be seen in the figures, the maximum cloud absorption over the spectral range of 10000 to 15000 cm^{-1} is mainly due to the cloud water vapor absorption.

Between 7500 cm^{-1} and 10000 cm^{-1}, the water vapor absorption is slightly larger than liquid water absorption. Almost all the cloud absorption at wavenumber below about 7000 cm^{-1} and elsewhere between the water vapor bands, is due to liquid water absorption. Cloud water vapor absorption dominates the total cloud absorption only in the water vapor absorption bands above 8000 cm^{-1}. The only region of equivalent absorption by liquid water is in the band

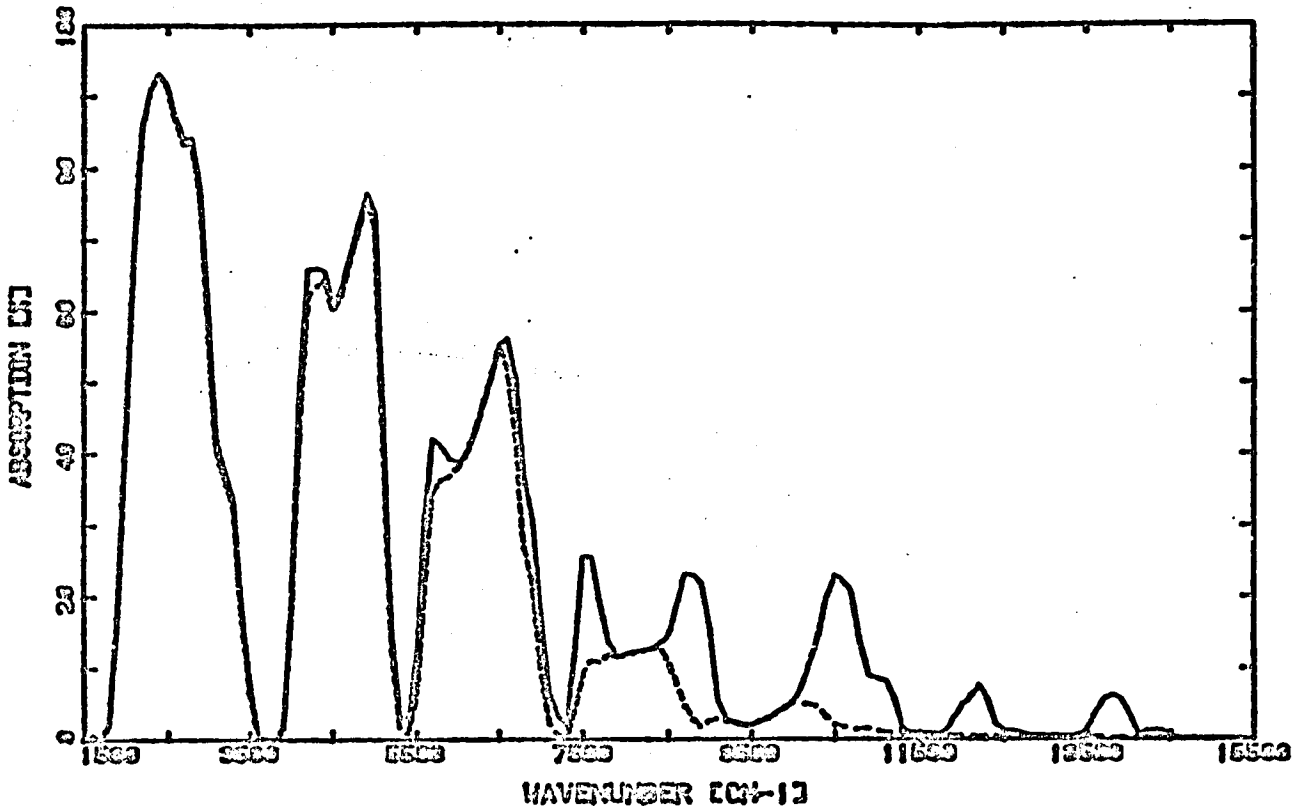

Figure 4.3 Fractional cloud absorption(solid) and liquid water absorption(dashed) as a function of wavenumber.

The same conditions in Fig. 4.1 are used.

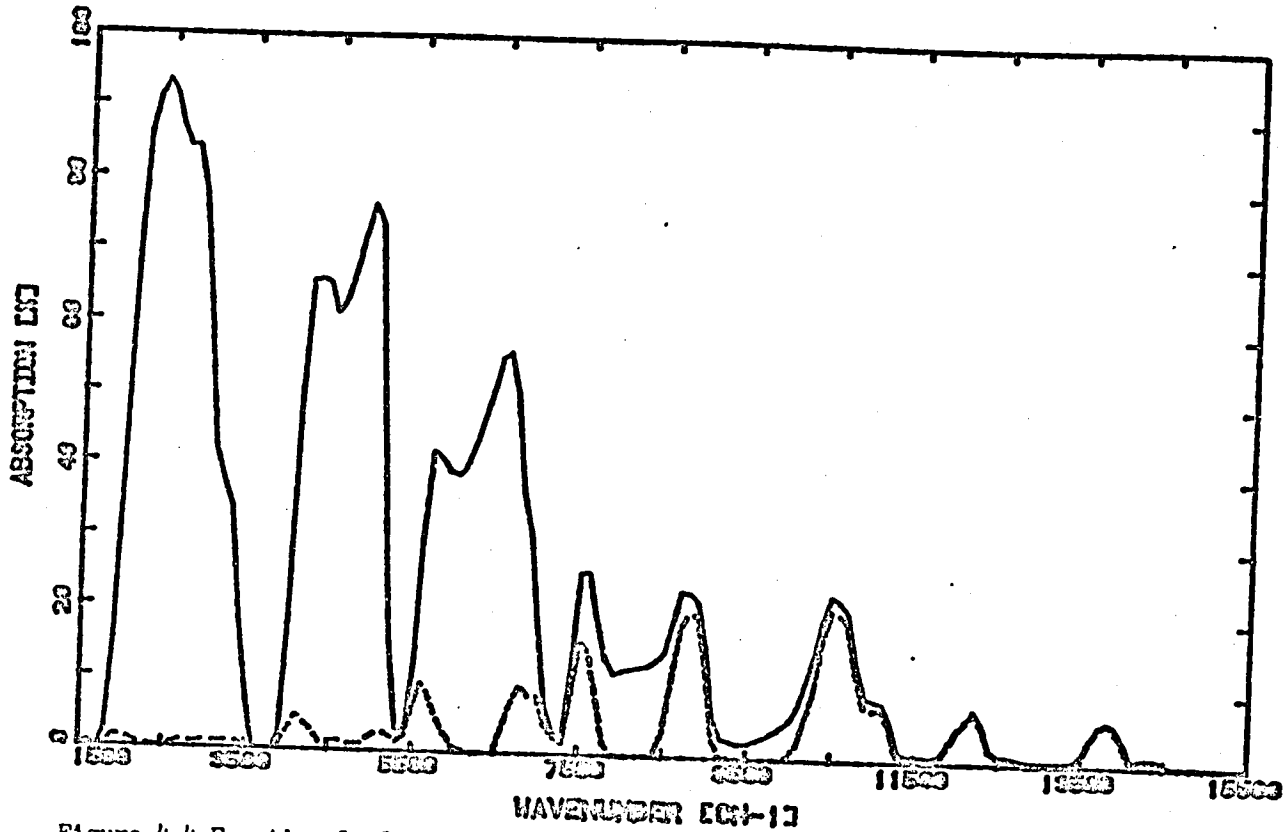

Figure 4.4 Fractional cloud absorption(solid) and cloud water vapor absorption (dashed) as a function of wavenumber.

The same conditions in Fig. 4.1 are used.

centered at 7500 cm^{-1}.

The above results for continuously variable absorption may be summarized discretely using the conventional water vapor absorption bands, namely: 0.7, 0.8, $\rho\sigma z$, Φ, Ψ, Ω, X and 3.2. Table 4.1 shows fractional absorption within and between the water vapor absorption bands due to water vapor and liquid water. The U.S. standard atmosphere(1962) and stratus cloud are used to estimate relative spectral absorption by water vapor and liquid water. The values in Table 4.1 are calculated as a percentage of incident spectral irradiance at the cloud top. The highest fractional absorption in a water vapor band is about 97 % in the 3.2 μm band, and the lowest fractional absorption is about 3 % in the 0.7 μm band. In terms of the contribution of each band to total cloud absorption, the Ψ and Ω bands are very dominant in Table 4.1. These two bands constitute about 35 % and together with the spectral band between them, make up almost 50 % of the total cloud absorption. As illustrated in Table 4.2, water vapor absorption is only dominant in the 0.7, 0.8, and $\rho\sigma z$ bands, while droplet absorption dominates elsewhere. As the cloud top is raised, the relative water vapor absorption decreases in each band. For the cloud top with height of 1.5 km, the extent of the cloud absorption in the eight bands occupies 69.7 % of total cloud absorption in the entire solar spectrum. For the relative absorption in the eight bands, liquid absorption

Table 4.1

Spectral Cloud Absorption within and between the Water Vapor Bands

Band Name	Band Interval ($\Delta\lambda$; μm)	$F_{\Delta\lambda}$(abs.) (W/m^2)	$\frac{F_{\Delta\lambda}(abs.)}{\Delta\lambda}$ ($Wm^{-2}\mu m^{-1}$)	$\frac{F_{\Delta\lambda}(abs.)}{F_{\Delta\lambda}}$ (%)	$\frac{F_{\Delta\lambda}(abs.)}{\text{Total abs.}}$ (%)
	0.20~0.70	0.25	0.50	0.04	0.20
0.7	0.70~0.74	1.66	41.5	3.23	1.32
	0.74~0.79	0.27	5.40	0.45	0.21
0.8	0.79~0.84	1.97	39.4	3.78	1.56
	0.84~0.86	0.19	9.50	0.96	0.15
$\rho\sigma z$	0.86~0.99	11.33	87.15	11.33	8.99
	0.99~1.03	1.30	32.50	4.44	1.03
Φ	1.03~1.23	12.31	61.55	11.96	9.77
	1.23~1.25	1.07	53.50	11.93	0.85
Ψ	1.25~1.54	24.18	83.38	40.65	19.18
	1.54~1.70	16.56	103.50	44.04	13.14
Ω	1.70~2.10	19.95	49.88	63.94	15.83
	2.10~2.27	8.77	51.59	65.16	6.96
χ	2.27~3.0	10.09	13.82	78.26	8.01
3.2	3.0~3.57	6.31	11.07	96.94	5.01
	3.57~7.0	9.83	2.87	92.50	7.80

$F_{\Delta\lambda}(W/m^2)$;Solar irradiance for a given band at the cloud top. The cloud is assumed to have 1 km thickness, and is in the U.S. standard atmosphere under overhead sun.

Table 4.2

Fractional Absorption of Stratus Cloud

(1) Case of Cloud Top Altitude of 1.5 km

Band Name	0.7	0.8	$\rho\sigma z$	ϕ	Ψ	Ω	χ	3.2
TOABS	3.2	3.8	11.3	12.0	40.7	63.9	78.3	96.9
WVABS	93.1	91.2	80.4	49.5	26.3	10.9	6.1	2.2
LWABS	6.9	8.8	19.6	50.6	73.6	89.1	94.0	97.8

(2) Case of Cloud Top Altitude of 5 km

Band Name	0.7	0.8	$\rho\sigma z$	ϕ	Ψ	Ω	χ	3.2
TOABS	1.3	1.6	6.8	9.6	43.4	65.0	81.6	95.8
WVABS	82.2	77.9	62.4	34.0	20.8	10.0	4.0	1.1
LWABS	17.8	22.1	37.6	66.0	79.2	90.0	96.0	98.9

The cloud is assumed to have 1 km thickness, and is in the U.S. standard atmosphere under overhead sun. TOABS; cloud absorption for each band. WVABS ; relative fractional water vapor absorption in cloud. LWABS ; relative fractional liquid water absorption in cloud. All values in Table 4.2 are expressed as percentages.

takes 68.3 % and water vapor absorption occupies 31.7 %. Outside the water vapor bands, liquid water contributes about 30 % of total cloud absorption.

As the height of cloud top changes from 1.5 km to 5 km, the total cloud absorption in the eight bands is increased about 3.1 %. This is due to greater absorption by the droplets. Of the absorption of eight bands, the liquid water now occupies 81.1 % while water vapor takes 18.9 %.

4.2 Comparison of the Results with a Previous Work

It is desirable to compare these results obtained from photon pathlength distribution with previous work. To examine the validity of computed results, the present work is compared with Welch and Cox (1980). Table 4.3 gives a comparison for a stratus cloud. Before examining the values in Table 4.3, it is important to point out that the present computation used the same type of drop size distribution and the same atmospheric model as the Welch and Cox study.

There appears to be a general agreement in the values of cloud transmission and absorption. However, there exist significant differences in the values of reflection and water vapor absorption above the cloud top. The values of water vapor absorption above the cloud can also be examined based on the absorptivity curve in Lacis and Hansen(1974). According to their curve, the water vapor amount yielding a

Table 4.3

Comparisons of the Present Work and Welch and Cox's Study

Cloud Top Height(km)		Present Work (%)	Welch and Cox (%)	Difference
	T	13.9	12.8	+1.1
1.5	R	65.9	58.7	+7.2
	A	8.0	8.0	0.0
	ATM	12.2	20.5	-8.6
	T	14.2	13.3	+0.9
4	R	67.9	62.1	+5.8
	A	9.1	10.7	-1.6
	ATM	8.8	13.9	-5.1
	T	14.9	14.2	+0.7
10	R	71.5	69.4	+2.1
	A	12.6	16.4	-3.8
	ATM	1.0	0.0	+1.0

A stratus cloud whose thickness is 1 km is embedded in an atmospheric model of GATE phase III with overhead sun. T; transmission, R ;reflection, A ; absorption, ATM; atmospheric water vapor absorption above the cloud.

fractional absorption of 20 % must be larger than 10 cm of precipitable water. It therefore appears that Welch and Cox grossly overestimated water vapor absorption above the cloud. This overestimation of water vapor amount above the cloud directly affects their reflection values. Unfortunately, there appears to be a lack of other published results for further independent verification of the model presented here.

4.3 Limitations of the Model

The present calculations are performed based on plane-parallel homogeneous clouds, and zero reflection of solar radiation from the earth's surface. Actually, clouds are finite in their dimension, and their drop size distribution depends on the position within cloud. In addition, cloud vapor density changes with height. The reflection of solar radiation from the surface affects cloud absorption. However, it is neglected in the present calculations because of its small effect on cloud absorption.

For the generation of photon pathlength distribution, the Monte Carlo method is used. A stochastic error is expected from the Monte Carlo simulation of multiple scattering. This error can be reduced by considering the number of histories and was small for the cases considered here. The stochastic error is about 0.1 % in the generation of photon

pathlength distribution.

The water vapor transmission function is obtained from LOWTRAN 5. The computer code of LOWTRAN 5 calculates atmospheric transmission averaged over 20 cm^{-1} intervals in steps of 5 cm^{-1} from 350 cm^{-1} to 40000 cm^{-1}. The code uses a single parameter band model for molecular absorption. In the case of the present calculations, some error is expected from the estimation of the water vapor transmission function because LOWTRAN 5 is incomplete. Although it is difficult to assess accurately the error originated in LOWTRAN 5, the error in the water vapor transmission function is expected to be less than 1 %.

4.4 Dependence of Absorption on Cloud Top Altitude

Figure 4.5 illustrates how the water vapor absorption above the cloud and the total cloud absorption depends on the cloud top altitude. A stratus cloud whose thickness is 1 km is assumed to be embedded in an atmospheric model for GATE phase III with overhead sun. The cloud top altitude changes from 1.5 to 10 km in the atmospheric model. As the height of the cloud top increases, absorption by water vapor above the cloud decreases rapidly due to less column vapor amounts, while liquid water absorption and total absorption increases steadily within the cloud due to an increase in the solar radiation incident on the cloud top. As the cloud top altitude increases, cloud temperature decreases and

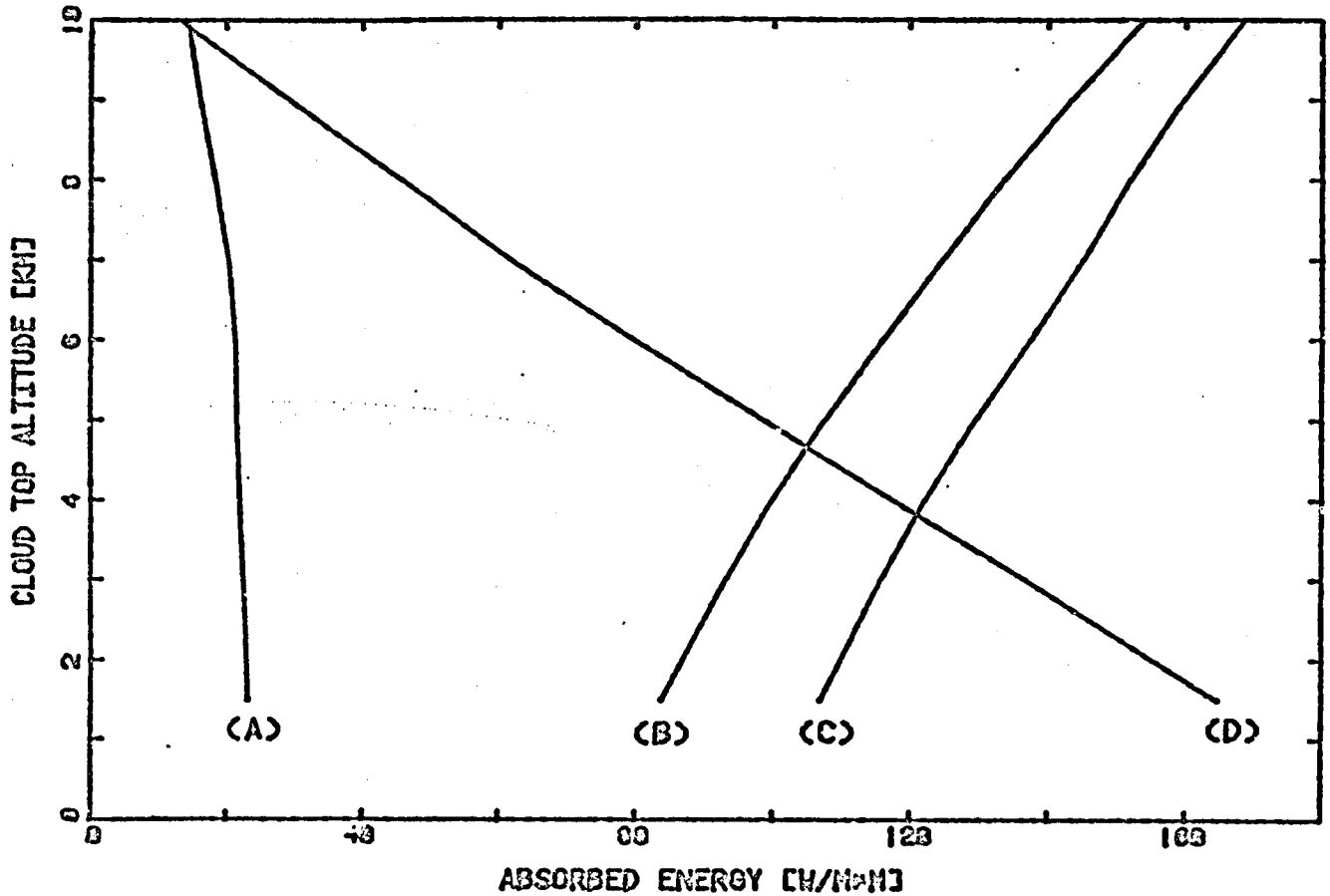

Figure 4.5 Water vapor absorption(A), droplet absorption(B), total cloud absorption(C), and column vapor absorption(D) versus cloud top altitude.

consequently the water vapor amount in the cloud decreases. Figure 4.5 does not show much decrease in cloud vapor absorption. This means that the reduced atmospheric water vapor absorption above the cloud largely compensates for the lower vapor density within the cloud.

At a height of 10 km, the total cloud absorption is increased about 57 % of its value at 1 km, and liquid water absorption is about 84 % higher. In contrast, the atmospheric water vapor absorption above the cloud is reduced about 92 % from its value at 1 km. Thus, water vapor absorption above the cloud has a very important effect on the calculation of total cloud absorption.

Figure 4.6 shows the spectral absorption by a stratus cloud and atmospheric water vapor above the cloud for the cloud top altitude of 2 km. The cloud whose thickness is 1 km is assumed to be embedded in an atmospheric model for GATE phase III with overhead sun. This figure illustrates the spectral cloud absorption and atmospheric water vapor absorption in energy per unit wavenumber. Figure 4.7 also shows the spectral cloud absorption and atmospheric absorption above a cloud for the cloud top altitude of 5 km. A comparison of Figures 4.6 and 4.7 shows that as the cloud top height increases, spectral cloud absorption increases steadily between 1500 and 7500 cm^{-1} while the atmospheric water vapor absorption above the cloud decreases

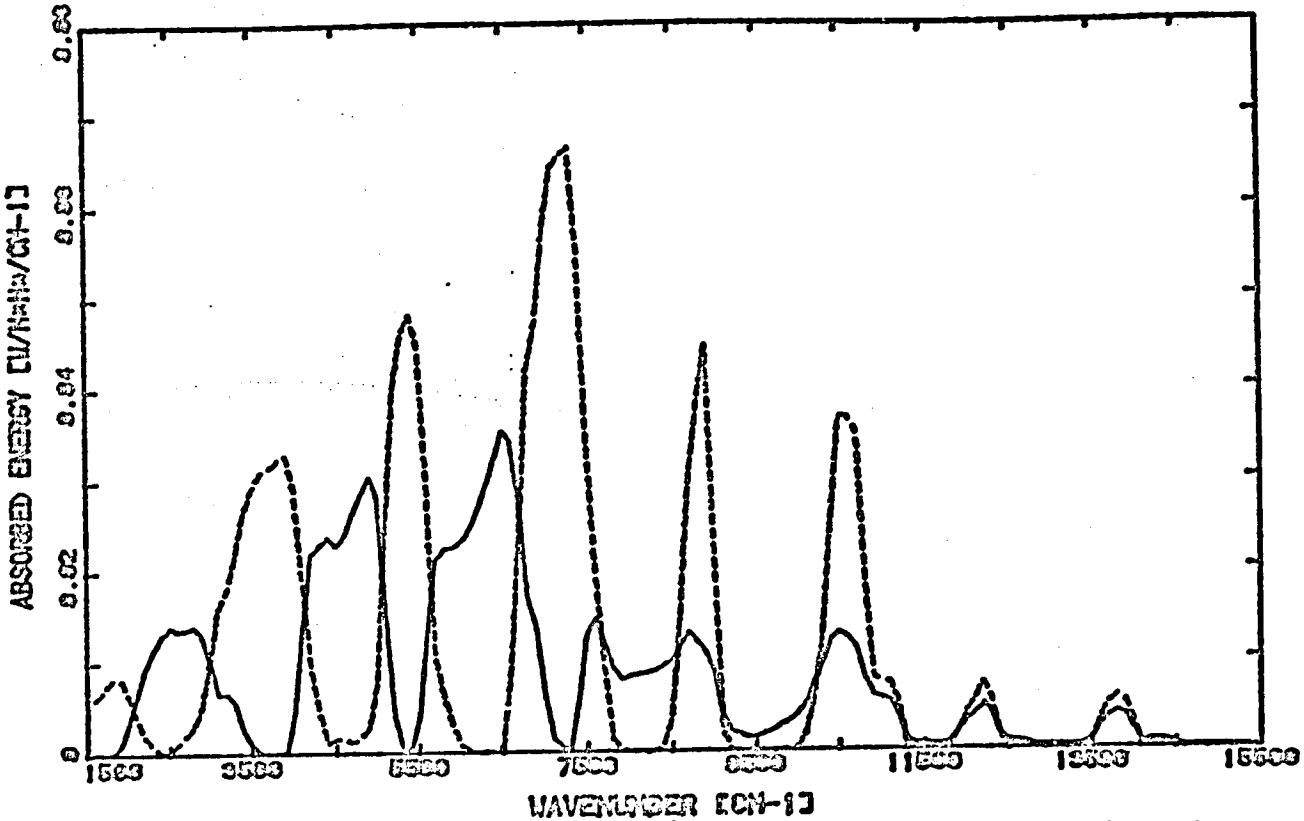

Figure 4.6 Spectral cloud absorption(solid) and atmospheric water vapor absorption (dashed) for cloud top altitude of 2 km.

The cloud is embedded in an atmospheric model for GATE phase III with overhead sun.

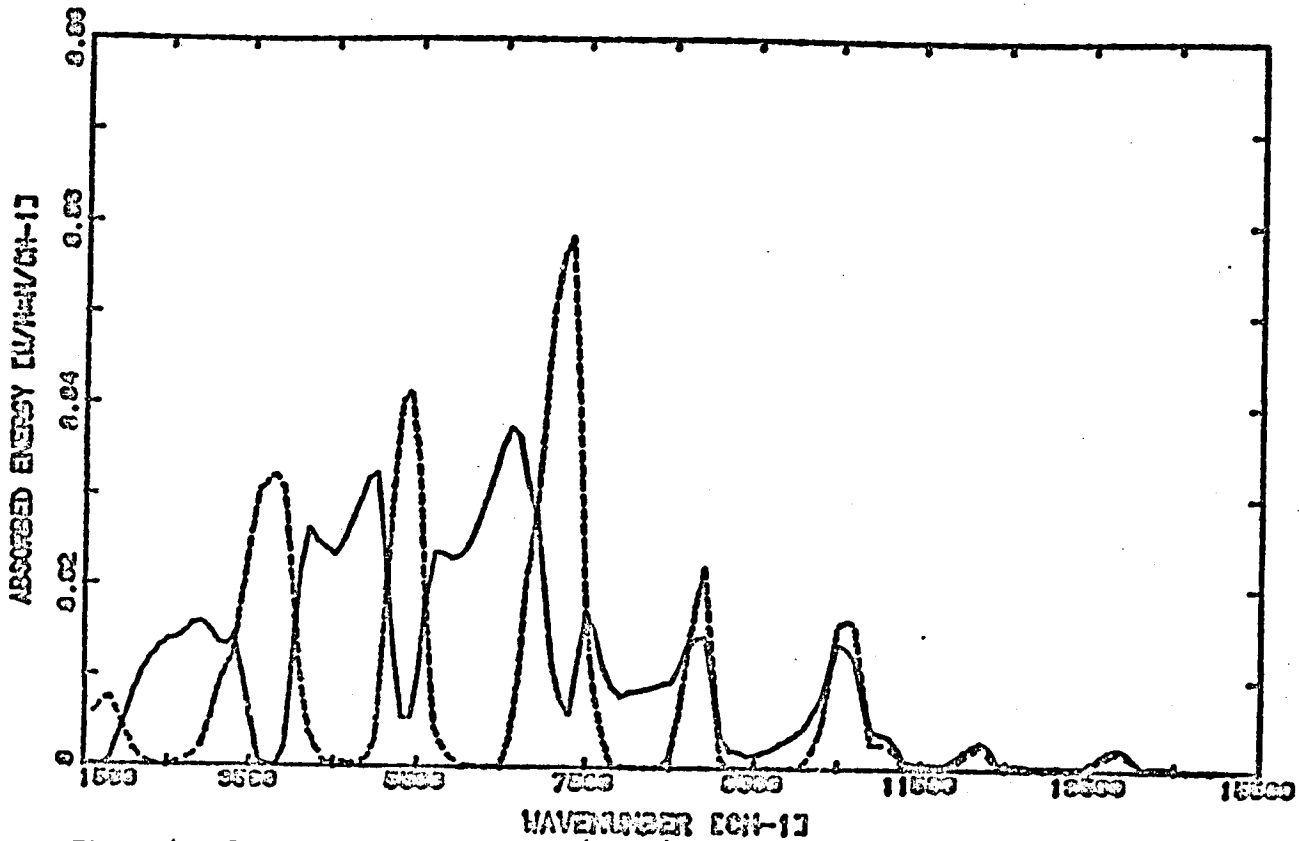

Figure 4.7 Spectral cloud absorption(solid) and atmospheric water vapor absorption (dashed) for cloud top altitude of 5 km.

The same conditions in Fig. 4.6 are used for solar zenith angle and atmospheric model.

significantly in the spectral region between 4500 and 11500 cm^{-1}. In the spectral region ranging from 10000 to 14000 cm^{-1}, both cloud absorption and column vapor absorption are decreased. Over this spectral range, cloud water vapor absorption dominates over liquid water absorption, and the decrease of cloud absorption is due to the decrease of water vapor amount within and above the cloud.

Figures 4.8 and 4.9 display liquid water absorption for cloud top altitudes of 2 km and 5 km, respectively. An increase in liquid water absorption can be seen from the comparision of Figures 4.8 and 4.9, as evidenced by the broadening of the liquid water absorption bands. A comparison of Figure 4.10 and 4.11 shows that as the cloud top altitude changes from 2 km to 5 km, the cloud water vapor absorption is decreased slightly everywhere except for the spectral region between about 4800 and 8000 cm^{-1}. For the change of cloud top altitude, two major factors are related to cloud water vapor absorption: (1) decrease of water vapor density in cloud due to the lower temperature, (2) increase of available solar energy for cloud absorption by the decrease of atmospheric vapor absorption above the cloud. Thus, the increase of spectral absorption between about 4800 and 8000 cm^{-1} may be explained by the more dominant effect of (2) over the effect of (1). The net effect of increase of cloud top altitude makes the cloud water vapor absorption decrease.

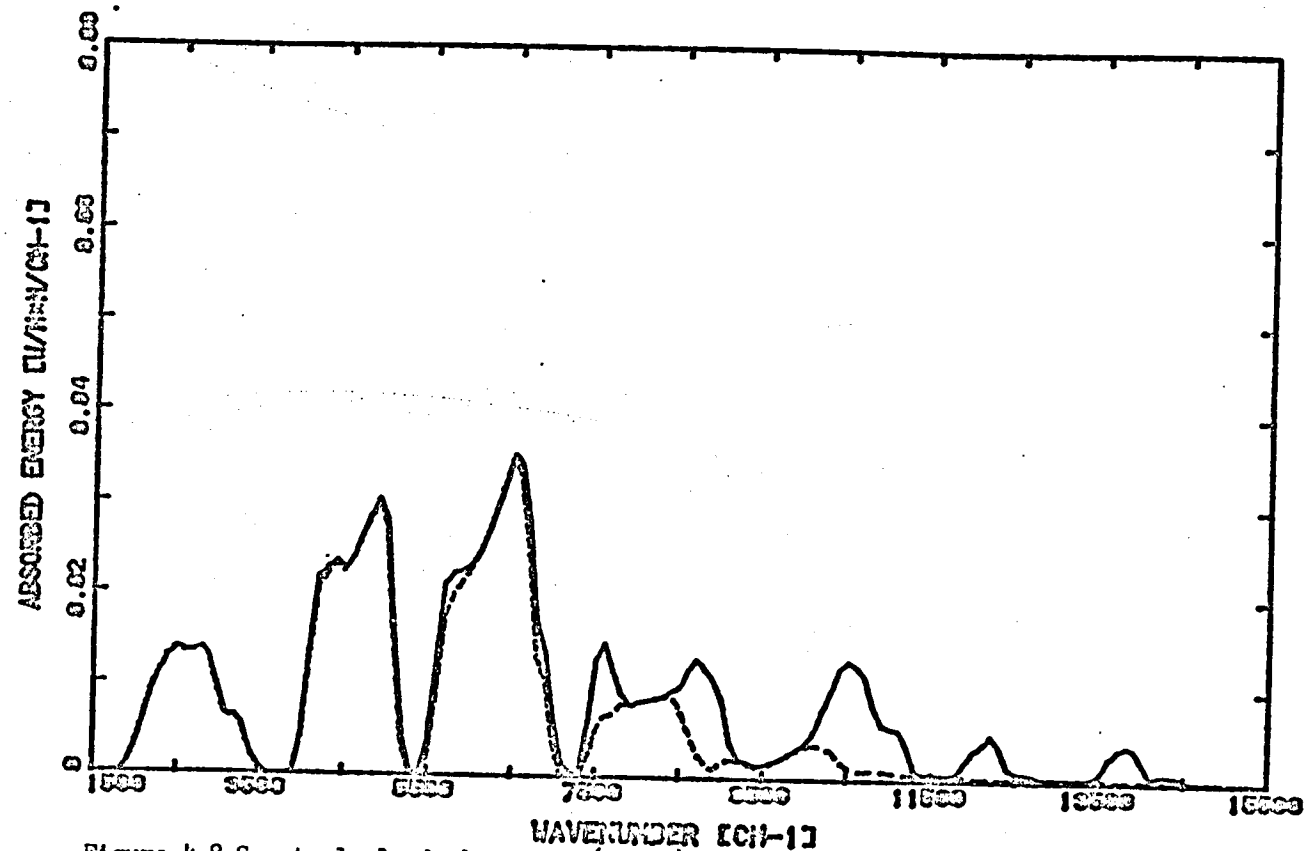

Figure 4.8 Spectral cloud absorption(solid) and liquid water absorption(dashed) for cloud top altitude of 2 km.

The cloud is embedded in an atmospheric model of GATE phase III with overhead sun.

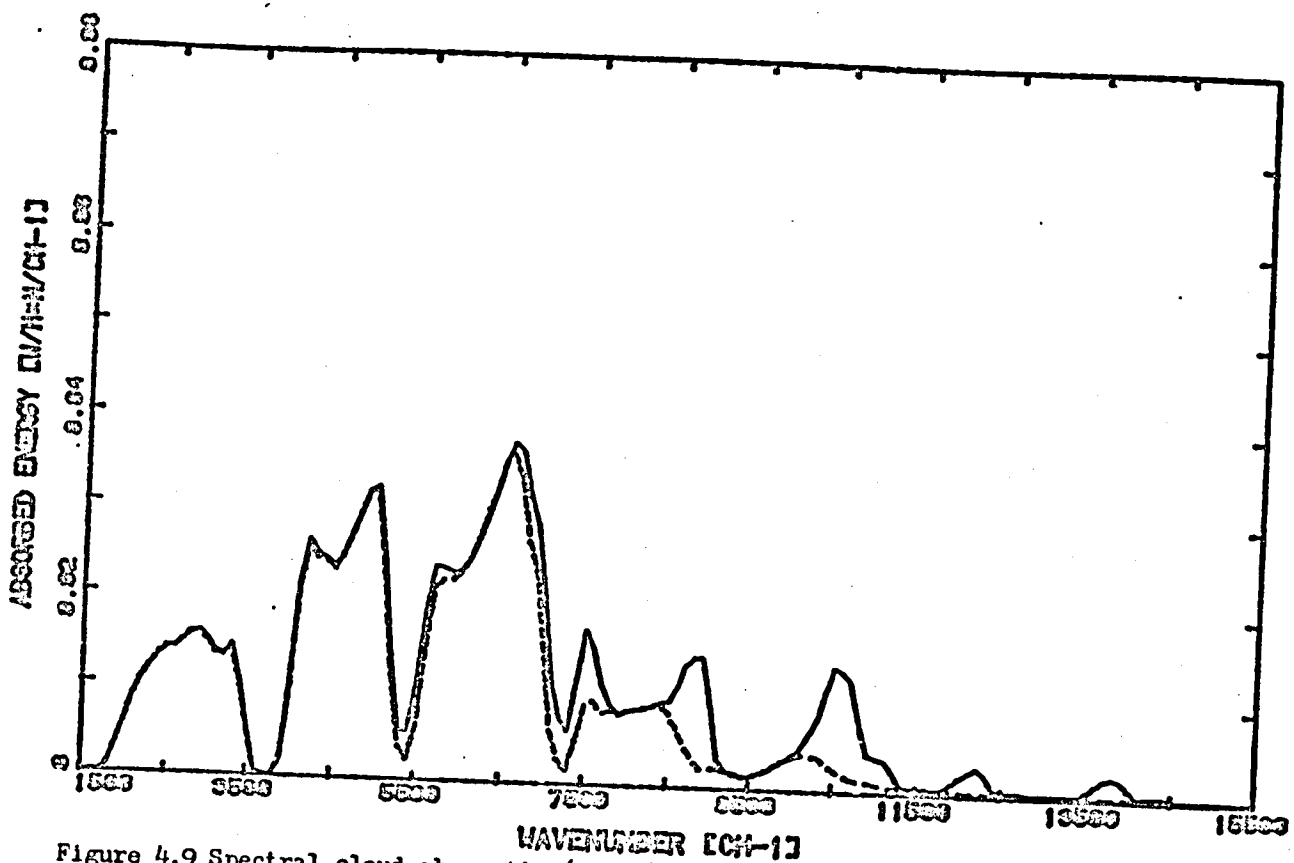

Figure 4.9 Spectral cloud absorption(solid) and liquid water absorption(dashed) for cloud top altitude of 5 km.

The cloud is embedded in an atmospheric model of GATE phase III with overhead sun.

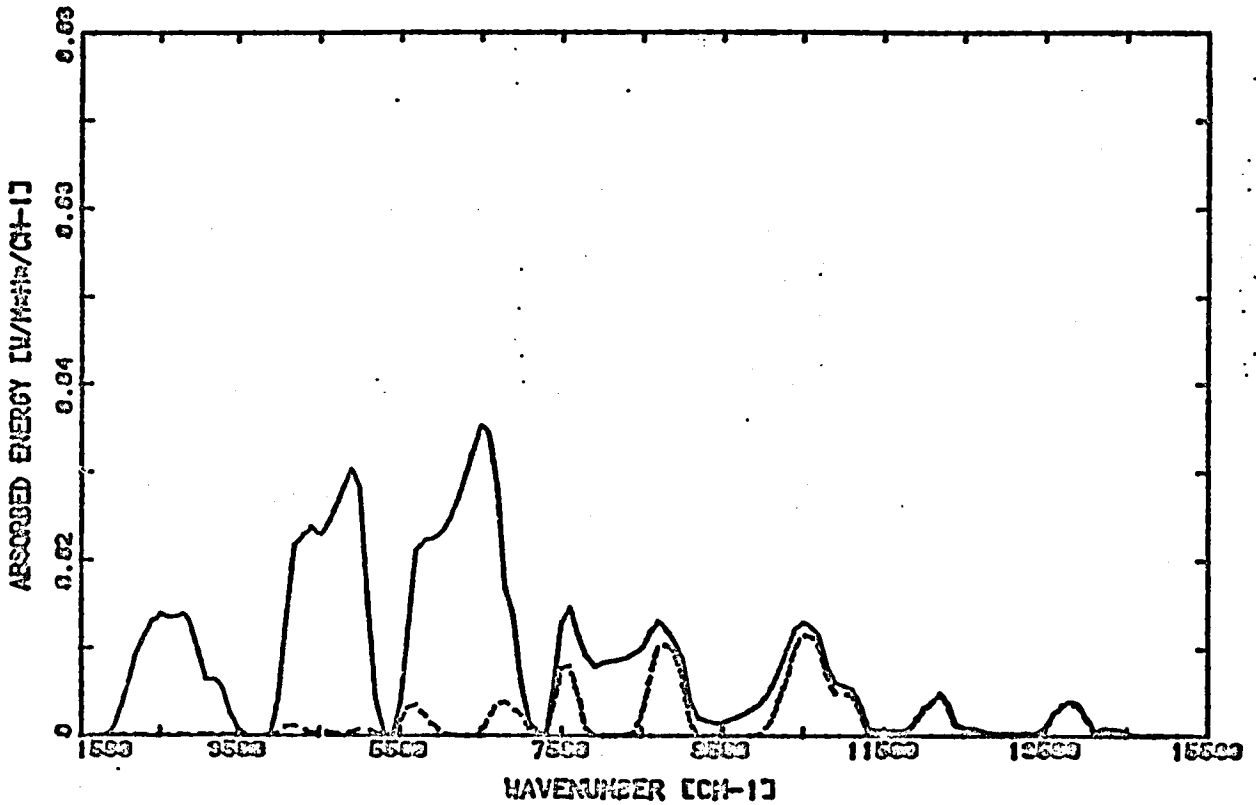

Figure 4.10 Spectral cloud absorption(solid) and cloud water vapor absorption (dashed) for cloud top altitude of 2 km.

The same conditions in Fig. 4.6 are used for solar zenith angle and atmospheric model.

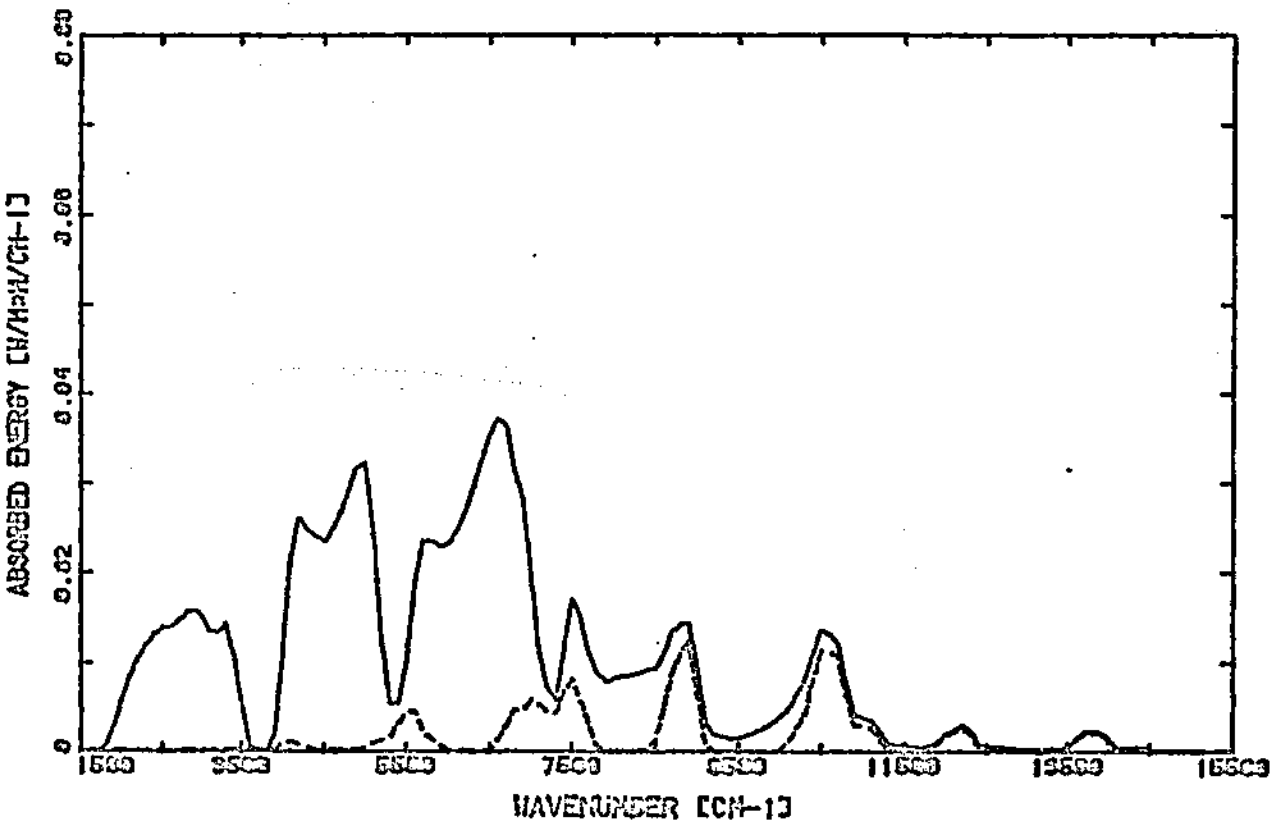

Figure 4.11 Spectral cloud absorption(solid) and cloud water vapor absorption (dashed) for cloud top altitude of 5 km.

The same conditions in Fig. 4.7 are used for solar zenith angle and atmospheric model.

4.5 Cloud Absorption for Different Atmospheric Models

Table 4.4 presents absorption, reflection, and transmission by stratocumulus cloud for five different atmospheric models. The values of cloud absorption are nearly constant except for GATE phase III. This exception can be explained by the higher moisture content of its atmospheric model, causing greater water vapor absorption above the cloud than for the other atmospheric models.

Conversely, Table 4.4 also shows the highest cloud absorption occurs for a the mid-latitude winter atmosphere. This is due to the lowest absorption of the water vapor above the cloud. In addition, the highest value of transmission and reflection for the same atmospheric model may be explained by the same reason. In contrast, the values in GATE phase III show that the lowest ones are due to the highest water vapor absorption above the cloud.

Thus, cloud absorption does not change significantly with the atmospheric models. However, the atmospheric water vapor absorption is strongly dependent on the moisture distribution of atmospheric models.

4.6 Change of Cloud Absorption with Cloud Thickness

Table 4.5 is an illustration of cloud absorption, reflection, and transmission with the change of geometrical

Table 4.4

Cloud Absorption for Different Atmospheric Models

	Standard atmos.	Tropical atmos.	Mid-lat. summer.	Mid-lat. winter	GATE phase III
Transmission	340.2	333.6	335.5	343.9	333.0
Reflection	790.7	775.9	780.5	799.0	771.9
Absorption	110.4	108.2	109.8	117.7	93.7
Atmospheric vapor abs.	93.9	117.8	109.5	80.4	137.1
Water vapor path	0.20	0.45	0.34	0.12	0.83

All values in Table 4.5 have units of W/m^2. A stratocumulus cloud is assumed to be embedded in the five different atmospheric models with overhead sun. The cloud top altitude is 3 km, and its thickness is 1 km. The vertical water vapor path above the cloud is expressed in cm.

Table 4.5

Cloud Absorption with Change of Cloud Thickness

ΔZ(km)	Percent	Stratocumulus	Nimbostratus
0.5	Transmission	28.2	8.6
(2.5~3)	Reflection	63.9	79.9
	Absorption	7.9	11.5
1	Transmission	27.9	8.5
(2~3)	Reflection	63.2	79.5
	Absorption	8.9	12.0
2	Transmission	27.3	8.4
(1~3)	Reflection	62.2	78.6
	Absorption	10.5	13.0

The clouds are assumed to be in the tropical atmosphere with overhead sun.

thickness of cloud. The calculations are performed for constant scattering optical thickness for each cloud discussed in section 3.2. The total liquid water content of clouds is kept fixed because of the uniform distribution of cloud droplets. The cloud top altitude is also fixed at 3 km so that all clouds may have the same amount of solar flux on their upper boundary.

Table 4.5 shows that as the cloud thickness increases, cloud absorption increases. In addition, the reflection and transmission show a slight decrease in their values as the geometrical cloud thickness increases. Therefore, it is obvious that the geometrical thickness of the cloud is not an important factor for fixed water content, but the optical thickness is a major factor in determining cloud absorption, reflection, and transmission.

4.7 Cloud Absorption by Different Types of Cloud

The cloud absorption depends to some extent upon the microphysical properties and stage of developmemt of cloud. Table 4.6 shows total absorption, reflection, and transmission for three types of cloud discussed in section 3.2. As can be seen from Table 4.6, the highest absorption takes place in the nimbostratus, which has the highest liquid water content.

Table 4.6

Cloud Absorption by Different Types of Cloud

percent	Stratus (top)	Stratocumulus (base)	Nimbostratus (top)
Absorption	10.5	8.7	11.9
Transmission	15.5	27.4	8.5
Reflection	74.0	63.9	79.6

Note; All clouds are assumed to be embedded in the atmospheric model of mid-latitude summer with overhead sun. The cloud top altitude is 2.5 km, and the thickness of clouds is 1 km. All values in Table 4.6 are expressed as percentages of solar radiation incident on the cloud top.

It appears that the amount of liquid water has little effect on cloud absorption. For example, the liquid water content of nimbostratus is about seven times larger than that of stratocumulus, but the difference in their fractional absorptions is only 3.2 %. On the other hand, the liquid water content strongly influences cloud reflection and transmission. In the case of transmission and reflection, the differences between these two cloud types are approximately 19 % and 16%.

4.8 Dependence of Cloud Absorption on Solar Zenith Angle

Based on the incident solar radiation at the top of cloud, the fractional absorption is plotted against the solar zenith angle in Figure 4.12. The height of the cloud top is assumed to be 3 km, and its thickness is 1 km. The U.S. standard atmospheric model and stratus cloud are used for the calculation of fractional absorption. The result indicates that the fractional absorption decreases from 10.7 % to 5.7 % as the solar zenith angle increases. However, this range is quite variable with the type of cloud, cloud thickness, and atmospheric state.

Figure 4.13 shows that the absorbed energy by stratus cloud decreases steadily with the increase of solar zenith angle for the same conditions as Figure 4.12. The cloud absorbs about 134 W/m^2 under overhead sun and about 13 W/m^2 for a solar zenith angle of 75°. The decrease in absorbed

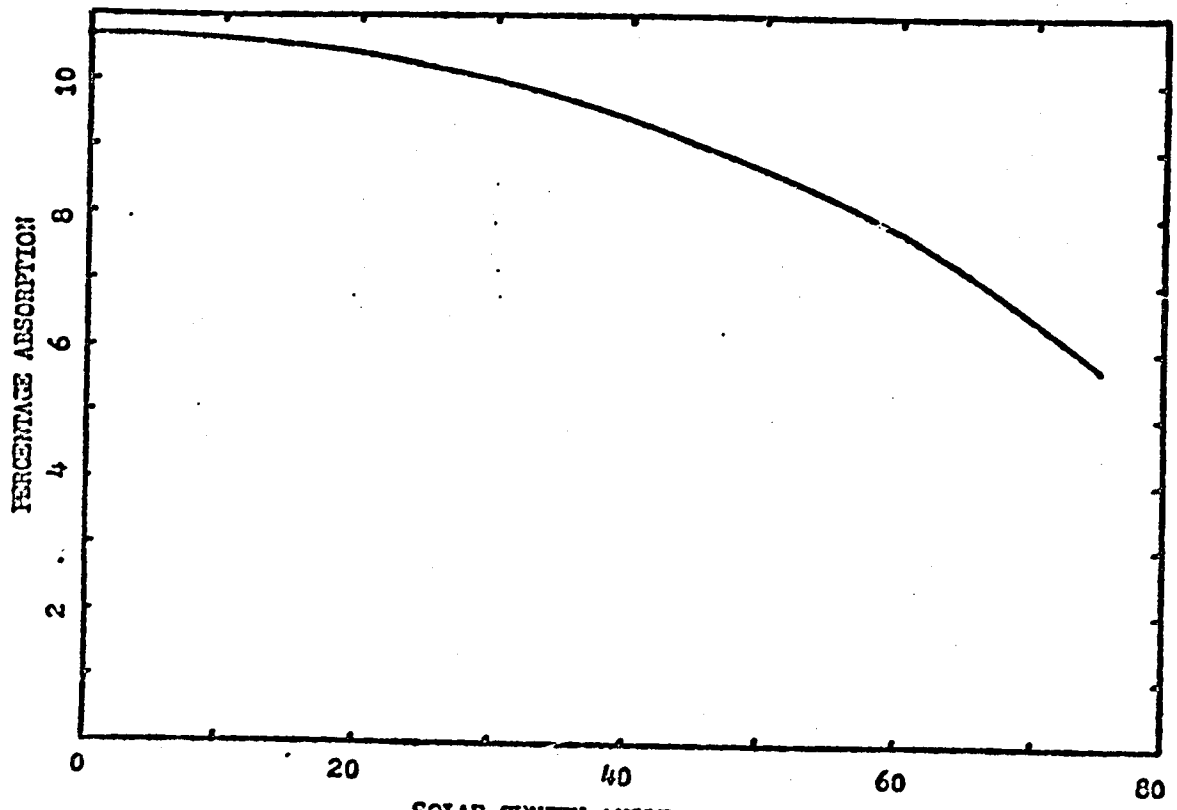

Figure 4.12 Fractional cloud absorption versus solar zenith angle.

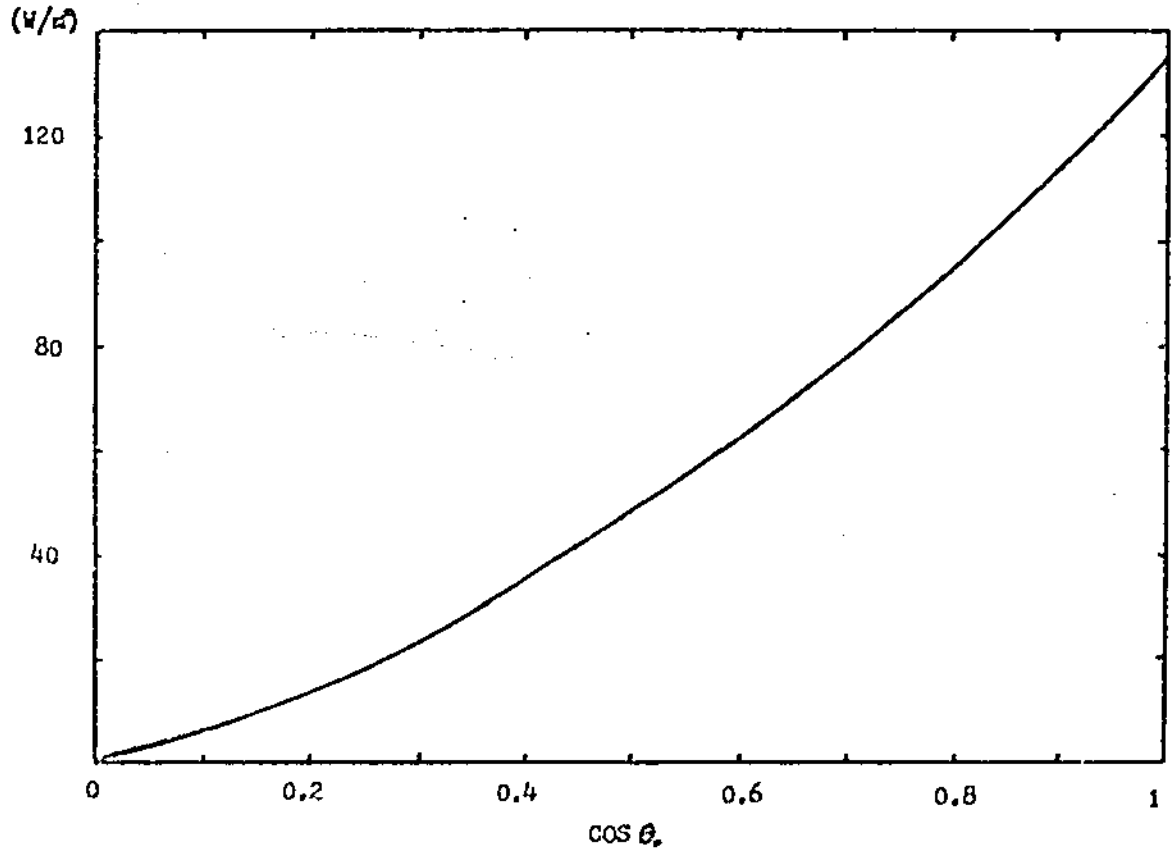

Figure 4.13 Cloud absorption versus cosine of solar zenith angle

energy may be explained by (1) decrease of incident solar energy per unit area due to effect of angle of incidence, and (2) shorter pathlength of photons due to less probability of penetration into cloud, and (3) increase of water vapor path above the cloud.

V. GLOBAL APPLICATION OF MODEL RESULTS

The results obtained in Chapter IV may be used in global applications; for example, general circulation or climate models. Since the energy absorbed, reflected, and transmitted by a cloud is not significantly dependent on the seasonal and zonal atmospheric models, it is possible to generate cloud absorption by a simple parameterization of the optical properties of cloud, based on cloud climatology. The atmospheric water vapor absorption above the cloud can also be obtained easily from the relevant atmospheric model. The results of Figure 4.5, in particular can be used as a useful guideline for the parameterization of cloud absorption and atmospheric water vapor absorption above the cloud. The nearly linear variation of these two curves will make parameterization simpler.

A range of cloud absorption under overhead sun may be suggested for global applications. The values in Table 5.1.(a) are only applicable to the clouds whose liquid water content ranges from 0.14 to 1.0 gram/m^3, and are given as the fraction of solar radiation at cloud top.

An estimation of cloud absorption can be made by the global averages of liquid water content and thickness of

Table 5.1

Global Application of Cloud Absorption Model

(a) Range of Global Cloud Absorption for Overhead Sun

Cloud Thickness(km)	Cloud absorption(%)
0.5	7 - 12
1	8 - 12
2	10 - 13

The values in Table 5.1.(a) are expressed as a fraction of solar radiation incident on the top of cloud.

(b) Zonal Average of Cloud Absorption

Latitude zone	$\langle COS\theta_0 \rangle$	$(CLDABS)_{MC}$ (W/m^2)	$\frac{(CLDABS)_{MC}}{F_0 \langle COS\theta_0 \rangle}$
0 ~ 10	0.634	59.2	6.9
10 ~ 20	0.615	56.9	6.8
20 ~ 30	0.577	51.6	6.6
30 ~ 40	0.521	48.2	6.8
40 ~ 50	0.450	42.8	7.0
50 ~ 60	0.365	34.6	7.0
60 ~ 70	0.269	25.5	7.0

The values in the last column are expressed as percentages. $(CLDABS)_{MC}$ is zonal average cloud absorption over daylength based on mean cosine of solar zenith angle. The subscript MC stands for mean cosine of θ_0. F_0 is solar irradiance at the top of the atmosphere. $\langle COS\theta_0 \rangle$ is mean cosine of solar zenith angle.

clouds. The global averages of liquid water content and cloud thickness may be assumed to be 0.2 - 0.3 g/m^3 and ~1.6 km. These values can be estimated approximately from a typical value of liquid water content of non-precipitating cumulus clouds, 0.5 g/m^3, and data on the zonal distribution of cloud amount and thickness (Paltridge and Platt,1976; Rogers,1979) Based on these values and Table 5.1.(a), liquid water clouds usually absorb about 8 - 9 % of the incident solar radiation at the top of cloud for overhead sun.

Based on the average cosine of solar zenith angle at the vernal equinox and the zonal distribution of cloud amount and thickness (Paltridge and Platt, 1976), Table 5.1.(b) illustrates an estimation of cloud absorption for each latitudinal zone in Northern Hemisphere. It is noted that the present calculations exclude the data on cirrus and altostratus clouds because these clouds are high-level clouds and are composed of ice crystals. Therefore, the values in Table 5.1.(b) are averaged ones due to only liquid water clouds. Although the result is a preliminary figure, the values in the last column show little variation with latitude zone. This may be explained by the fact that the mean water vapor path to cloud top is approximately independent of the latitudes. Approximately, the same mean water vapor path may be expected in both low and high latitudes since lower column vapor amount occurs at latitudes with higher mean solar zenith angle, and higher

column vapor amount takes place at latitudes with lower mean solar zenith angle.

Averaging cl[illegible] absorption from the equator to 70°N, the global average absorption is obtained and the value is estimated as about 47 W/m^2. This value is approximately 7 % of the globally averaged solar irradiance at the top of the atmosphere. However, this value may be changed by the consideration of ice crystal clouds.

VI. CONCLUSIONS

A theoretical model of spectral absorption of solar radiation in homogeneous clouds has been developed for the purpose of the present investigations. This model is limited to plane-parallel homogeneous water droplet clouds.

The model results presented in Chapter IV indicate that cloud absorption and atmospheric water vapor absorption above the cloud are highly dependent upon the wavenumber. There are four principal regions of minimum cloud absorption and three dominant bands of cloud absorption between about 1500 cm^{-1} and 7500 cm^{-1}. The three dominant cloud absorption bands exist at the points of the minimum atmospheric water vapor absorption, and are due to nearly complete liquid water absorption. The minimum cloud absorption regions are mainly due to the nearly complete absorption by atmospheric water vapor above the cloud. Over this spectral range, there is a general correspondence between the maximum cloud absorption and the minimum atmospheric water vapor absorption. Two cloud absorption bands between 7500 cm^{-1} and 11500 cm^{-1} occur at the points of the weak atmospheric water vapor absorption, and are mainly due to both liquid water and cloud water vapor absorption. The cloud absorption

bands between 11500 cm^{-1} and 15500 cm^{-1} are mainly due to water vapor absorption. Therefore, the liquid water contributes nearly completely to cloud absorption between 2000 cm^{-1} and 7500 cm^{-1} while water vapor absorption is the major contributor to cloud absorption between 10000 cm^{-1} 15000 cm^{-1}.

Averaged over the whole solar spectrum, total cloud absorption, as a fraction of the incident solar radiation at the top of the cloud, depends most strongly on liquid water absorption in the wavenumber interval ranging from 1800 to 11500 cm^{-1}, and to a lesser extent on water vapor absorption elsewhere. Thus, the most critical parameters to the model are liquid water content and the amount of water vapor above the cloud.

For the whole spectral range of solar radiation, 1 km thick cloud absorbs about 8 to 12 % of solar radiation incident on the cloud top for overhead sun. Cloud reflection changes from 12 % to 80 %, and transmission changes from 8.5 % to 28 %. In terms of the relative absorption by liquid water compared with water vapor within cloud, liquid water contributes about 77 % to 91 % of total cloud absorption, depending on cloud type, cloud top altitude, and atmospheric model. The cloud water vapor contributes the remaining 9 to 21 % to total cloud absorption. This relative ratio is sensitive to the changes

of cloud top altitude within the wavenumber interval of 8000 to 15000 cm^{-1}.

Water vapor absorption dominates over liquid water absorption in three bands, ie., 0.7, 0.8, and $\rho\sigma z$. The results obtained indicate that even in the water vapor absorption bands liquid water dominates over water vapor in absorption. Of the water vapor absorption bands, 3.2 μm band is the most highly saturated band, and ν band makes the highest contribution to total amount of energy absorbed by cloud.

For an increase in cloud top height, cloud and liquid water absorption increase significantly, while water vapor absorption decreases slightly. The cloud absorption does not show a significant difference for seasonal and zonal atmospheric models.

As the physical thickness of the cloud increases for fixed scattering optical thickness, fractional cloud absorption increases slightly while fractional cloud reflection and transmission show a slight decrease in their values.

The amount of liquid water in a cloud does not greatly influence fractional absorption of cloud. However, fractional transmission and reflection of cloud are highly dependent upon the liquid water content. For an increase of solar zenith angle, fractional cloud absorption and

transmission decreases steadily while cloud reflection increases. In the case of a stratus cloud whose thickness is 1 km, the range of fractional absorption decrease from 10.7 % to 5.7 %. for a change of solar zenith angle from zero to 75°.

The application of model results to global average liquid water content and thickness of cloud indicates that liquid water clouds absorb about 8 to 9 % of the incident solar radiation at the top of cloud under overhead sun. There are no strong zonal effects on fractional cloud absorption. The global mean fractional cloud absorption is about 7 % of the globally averaged solar irradiance at the top of atmosphere. However, this is an approximate estimation based on the data of liquid water clouds in the Northern Hemisphere.

Finally, the present results suggest that the amount of energy absorbed by a cloud is mainly determined by the liquid water content of the cloud, the atmospheric water vapor profile above the cloud top,and solar zenith angle. The liquid water absorption is primarily responsible for the cloud absorption, and increases with the increase of cloud top altitude. The cloud water vapor absorption is nearly constant for the change of cloud top altitude. As the cloud top altitude increases, the relative contribution of cloud

water vapor decreases while the liquid water absorption absorption increases.

Since the present work is limited to plane-parallel homogeneous clouds, future studies on this problem should include the effects of finite and inhomogeneous clouds, and should account for the global distribution of clouds. In addition, the effect of surface albedo in the presence of broken clouds has to be considered.

REFERENCES

REFERENCES

Appleby J.F., and W.M. Irvine, 1973: Path-length Distributions of Photons Diffusely Reflected from a Semi-infinite Atmosphere. Astrophys.,J.,183,337-346.

Bakan,S., and H. Quenzel,1976: Path Length Distributions of Photons Scattered in Turbid Atmosphere. Beitr. Phys. Atmos., 49, 272-278.

Bakan S., P. Koepke and H. Quenzel, 1978: Radiation Calculations in Absorption Bands: Computation of Exponential Series and Path Length Distribution-Method. Beitr. Phy. Atmos., 51, 28-30.

Clark,W,C,1982: Carbon Dioxide Review ;1982, Oxford University Press, New York, 469pp.

Danielson R.E,D.R. Moore and H.C Van de Hulst, 1969: The Transfer of Visible Radiation through Clouds. J. Atmos. Sci., 27, 1078-1087.

Davies,R.,1978: The Effect of Finite Geometry on the Three Dimensional Transfer of Solar Irradiance in Clouds. J. Atmos. Sci., 35,1712-1725.

Hale,G.M.,and M.R. Querry,1973:Optical Constants of Water in the 700-nm to 200-nm Wavelength Region Appl. Opt., 12, 555-563.

Herman,G.F.,1977: Solar Radiation in Summer Time Arctic Stratus Clouds. J. Atmos. Sci., 34, 1423-1432.

Irvine,W.M.,1964:The Formation of Absorption Bands and the Distribution of Photon Optical Paths in a Scattering Atmosphere. Bull. Astron. Ins. Neth., 17, 266-279.

Irvine,W.M.,1968:Diffude Reflection and Transmission by Cloud and Dust Layers. J. Quant. Spectrosc. Radiat. Transfer., 8, 471-485.

Irvine,W.M., and J.B. Pollack,1968: Infrared Optical Properties of Water and Ice Spheres, Icarus,8,324-366.

Kneizys,F.X., E.,P. Shettle, W.D. Gallery, J.H. Chetwynd, Jr., L.W. Aveu, J.E.A. Selby, R.W. Fenn, and R.A. McClatchey,1980:Atmospheric Transmittance/ Radiance: Computer Code LOWTRAN 5. AFGL-TR-80-0067, Air Force Geophysics Lab., Bedford, Mass.

Kransnokotskaya L.D.,and L.,M., Romanova,1974: Reflection, Transmission, and Absorption of Radiation by Clouds in the Absorption Bands of Water Vapor. NASA Technical Translation F-790 72-77.

Lacis,A.A. and J.E. Hansen,1974: A Parameterization of Absorption of Solar Radiation in the Earth's Atmosphere. J. Atmos. Sci., 31, 118-133.

Liou, K.N.,1976: On the Absorption, Reflection, and Transmission of Solar Radiation in Cloudy Atmosphere. J. Atmos. Sci., 33, 798-805.

Liou, K.N.,1980: An Introduction to Atmospheric Radiation. Academic Press.New York. 392pp.

McCartney,E.J.,1976:Optical Properties of the Atmosphere. Wiley, 408pp.

McClatchey,R.A, R.W. Fenn, J.E.A. Selby. F.E.Volz and J.S. Garing, 1972: Optcial Properties of the Atmosphere. 3rd ed. AFCRL-720467. Air Force Cambridge Research Lab., 107pp.

Paltridge,G.W., and C.M.R. Platt,1976: Radiative Processes in Meteorology and Climatology, Elsevier, 318pp.

Reynolds,D.W., T.H. Vonder Haar and S.K. Cox,1975: The Effect of Solar Radiation Absorption in the Tropical Atmosphere Atmosphere. J. Appl. Meteor., 14, 433-444.

Rogers,R.R.,1979: A Short Course in Cloud Physics. Pergammon Press, 235pp.

Sasamori,T, J. London and D.V,Hoyt,1972: Radiation Budget of the Southern Hemisphere. Meteor. Monogr., 13,No.35, 9-23.

Slingo A., and H.M., Schrecker,1982: On the Short Wave Radiative Properties of Stratiform Water Clouds. Quart. J. R. Met. Soc., 108, 407-426.

Stephens, G.L,1978: Radiation Profiles in Extended Water Clouds. I :Theory. J. Atmos. Sci., 35, 2111-2122.

C-2

Tampieri, F. and C. Tomasi,1976:Size Distribution Models of Fog and Cloud Droplets in Terms of the Modified Gamma Function. Tellus, 28, 333-347.

Thekaekara,M.P. and A.J. Drummond,1971: Standard Values for the Solar Constant and its Spectral Components. Nature(London), Phys. Sci., 229, 6-9.

Twomey, S.,1976: Computations of the Absorption of Solar Radiation by Clouds. J. Atmos. Sci., 33, 1087-1091.

Van de Hulst,H.C,1980:Multiple Light Scatterings, Tables, Formulas and Application. Academic Press. New York Vol. I and II, 739pp.

Van de Hulst H.C,1981:Light Scattering by Small Particles, Dover Publications,Inc., New York 470pp.

Welch,R.,M., J.F.Geleyn,W.G. Zdunkowski and G. Korb, 1976: Radiative Transfer of Solar Radiation in Model Clouds. Beitr. Phys. Atmos., 49, 128-146.

Welch,R,M. and S.K. Cox,1980: Solar Radiation and Clouds. Meteor. Monogr., 17,No.39, 3-20.

Wiscombe,W.J. and J.E. Evans,1977:Exponential-sum Fitting of Radiative Transmission Functions. J. Comput. Phys., 24, 416-444.

Wiscombe,W.J.,1979:Mie scattering calculations: Advances in Technique and Fast, Vector-speed Computer Codes. NCAR Tech. Note.-140+STR. 62pp.

Zdunkowski W.G. and R.F. Strand, 1969: Scattering Constants for a Water Cloud. Pure and Appl. Geophys., 19, 110-132.

END

DATE

FILMED

MAR 28 1984